The Canadian Mineralogist
Vol. 35, pp. 397-423 (1997)

PRIMITIVE MAGMAS AT FIVE CASCADE VOLCANIC FIELDS: MELTS FROM HOT, HETEROGENEOUS SUB-ARC MANTLE

CHARLES R. BACON[1], PEGGY E. BRUGGMAN, ROBERT L. CHRISTIANSEN, MICHAEL A. CLYNNE, JULIE M. DONNELLY-NOLAN AND WES HILDRETH

U.S. Geological Survey, 345 Middlefield Road, Menlo Park, California 94025-3591, U.S.A.

ABSTRACT

Major and trace element concentrations, including *REE* by isotope dilution, and Sr, Nd, Pb, and O isotope ratios have been determined for 38 mafic lavas from the Mount Adams, Crater Lake, Mount Shasta, Medicine Lake, and Lassen volcanic fields, in the Cascade arc, northwestern part of the United States. Many of the samples have a high Mg# [$100Mg/(Mg + Fe^T) > 60$] and Ni content (>140 ppm) such that we consider them to be primitive. We recognize three *end-member* primitive magma groups in the Cascades, characterized mainly by their trace-element and alkali-metal abundances: (1) High-alumina olivine tholeiite (HAOT) has trace element abundances similar to N-MORB, except for slightly elevated *LILE*, and has Eu/Eu* > 1. (2) Arc basalt and basaltic andesite have notably higher *LILE* contents, generally have higher SiO_2 contents, are more oxidized, and have higher Cr for a given Ni abundance than HAOT. These lavas show relative depletion in *HFSE*, have lower *HREE* and higher *LREE* than HAOT, and have smaller Eu/Eu* (0.94–1.06). (3) Alkali basalt from the Simcoe volcanic field east of Mount Adams represents the third end-member, which contributes an intraplate geochemical signature to magma compositions. Notable geochemical features among the volcanic fields are: (1) Mount Adams rocks are richest in Fe and most incompatible elements including *HFSE*; (2) the most incompatible-element depleted lavas occur at Medicine Lake; (3) all centers have relatively primitive lavas with high *LILE/HFSE* ratios but only the Mount Adams, Lassen, and Medicine Lake volcanic fields also have relatively primitive rocks with an intraplate geochemical signature; (4) there is a tendency for increasing $^{87}Sr/^{86}Sr$, $^{207}Pb/^{204}Pb$, and $\delta^{18}O$ and decreasing $^{206}Pb/^{204}Pb$ and $^{143}Nd/^{144}Nd$ from north to south. The three end-member Cascade magma types reflect contributions from three mantle components: depleted sub-arc mantle modestly enriched in *LILE* during ancient subduction; a modern, hydrous subduction component; and OIB-source-like domains. Lavas with arc and intraplate (OIB) geochemical signatures were erupted close to HAOT, and many lavas are blends of two or more magma types. Pre-eruptive H_2O contents of HAOT, coupled with phase-equilibrium studies, suggest that these magmas were relatively dry and last equilibrated in the mantle wedge at temperatures of ~1300°C and depths of ~40 km, virtually at the base of the crust. Arc basalt and basaltic andesite represent greater extents of melting than HAOT, presumably in the same general thermal regime but at somewhat lower mantle separation temperatures, of domains of sub-arc mantle that have been enriched by a hydrous subduction component derived from the young, relatively hot Juan de Fuca plate. The primitive magmas originated by partial melting in response to adiabatic upwelling within the mantle wedge. Tectonic extension in this part of the Cascade arc, one characterized by slow oblique convergence, contributes to mantle upwelling and facilitates eruption of primitive magmas.

Keywords: arc magmatism, primitive basalt, geochemistry, isotopes, trace elements, Cascades, northwestern United States.

SOMMAIRE

Nous avons déterminé la concentration des éléments majeurs et des éléments traces, y compris les terres rares, par dilution d'isotopes, ainsi que les rapports des isotopes de Sr, Nd, Pb et O, de 38 échantillons de laves mafiques des suites volcaniques de Mount Adams, Crater Lake, Mount Shasta, Medicine Lake, et Lassen, dans l'arc des Cascades, dans le nord-ouest des États-Unis. Plusieurs des échantillons ont une valeur élevée de Mg# [$100Mg/(Mg + Fe^T) > 60$] et une teneur élevée en Ni (>140 ppm), de sorte que nous leurs attribuons un caractère primitif. Nous préconisons l'existence de trois pôles de magmas primitifs dans les Cascades, que distinguent les concentrations en éléments traces et en alcalins. (1) Les tholéiites à olivine riches en Al (HAOT) possèdent des concentrations en éléments traces semblables à celles des basaltes normaux des rides océaniques (N-MORB), sauf pour un léger enrichissement en éléments lithophiles à large rayon (*LILE*), et montrent un rapport Eu/Eu* supérieur à 1. (2) Les basaltes d'arc et les andésites basaltiques possèdent une concentration nettement plus élevée en *LILE*, et sont en général plus siliceux, plus oxydés, et contiennent plus de Cr pour une teneur en Ni donnée que HAOT. Ces laves montrent en plus un appauvrissement en éléments à large rapport de valence à rayon (*HFSE*), des teneurs en terres rares lourdes plus faibles et en terres rares légères plus élevées que HAOT, et un rapport Eu/Eu* plus faible (0.94–1.06). (3) Le basalte alcalin de la suite de Simcoe, à l'est de Mount Adams, un troisième pôle, contribue une signature géochimique "intraplaque" aux compositions de magmas. Parmi les caractéristiques géochimiques notables de ces suites volcaniques, signalons que (1) les roches de Mount Adams sont les plus riches en Fe et en la plupart des éléments incompatibles, y compris les *HFSE*, (2) les laves les plus appauvries en éléments incompatibles se trouvent à Medicine Lake, (3) tous les centres contiennent des laves relativement primitives, ayant

[1] *E-mail address*: cbacon@mojave.wr.usgs.gov

des rapports *LILE/HFSE* élevés, mais seuls les centres volcaniques de Mount Adams, Lassen, et Medicine Lake contiennent des roches relativement primitives ayant une signature géochimique "intraplaque", et (4) $^{87}Sr/^{86}Sr$, $^{207}Pb/^{204}Pb$, et $\delta^{18}O$ tendent à augmenter, et $^{206}Pb/^{204}Pb$ et $^{143}Nd/^{144}Nd$ tendent à diminuer, du nord vers le sud. Les trois pôles identifiés parmi les magmas des Cascades témoignent de l'implication de trois composantes dans le manteau: un manteau appauvri en dessous de l'arc, et modestement enrichi en *LILE* pendant un stade de subduction plus ancien, une composante représentant la plaque contemporaine, hydratée, en subduction, et un manteau ressemblant à la source des basaltes des îles océaniques. Des venues de magma ayant une signature géochimique typique d'un milieu d'arc et d'autres typiques d'un milieu intraplaque sont mises en place à proximité de venues HAOT, et plusieurs laves sont en fait un mélange d'au moins deux sortes de magma basaltique. D'après les teneurs en H_2O des venues HAOT avant leur éruption, considérées avec les résultats d'études de l'équilibre des phases, ces magmas étaient relativement secs, et ils se sont équilibrés en dernier lieu dans le coin de manteau par dessus la zone de subduction à environ 1300°C et à une profondeur d'environ 40 km, donc près de la base de la croûte. Les venues de basalte d'arc et d'andésite basaltique représenteraient des taux de fusion plus élevés que pour le cas de HAOT, présumément dans le même contexte thermique mais à une température de séparation plus faible, dans des domaines du manteau en dessous de l'arc qui avaient été enrichis par une composante hydratée venant de la subduction de la plaque Juan de Fuca, relativement jeune et chaude. Les magmas primitifs ont pris naissance par fusion partielle en réponse à une remontée dans le coin du manteau. Une extension tectonique dans cette partie de l'arc des Cascades, due à une convergence lente et oblique, a contribué à la montée du manteau et a facilité l'éruption des venues de magmas primitifs.

(Traduit par la Rédaction)

Mots-clés: magmatisme d'arc, basalte primitif, géochimie, isotopes, éléments traces, Cascades, nord-ouest des États-Unis.

Introduction

The major goal of this study is to "see through" effects of differentiation and contamination in order to establish mantle characteristics and melting processes beneath the Cascades (Fig. 1) by selecting phenocryst-poor samples of chemically primitive lava that approximate liquid compositions. We consider rocks *primitive* if they are rich in Mg relative to Fe, have high concentrations of compatible trace elements, and low contents of phenocrysts (generally <5%). In extreme cases, primitive lavas may approach compositions of primary magmas, in which ferromagnesian phenocrysts have mantle-compatible compositions, but in most of our examples, the designation *primitive* merely indicates that a sample is one of a particular eruptive unit that has been least modified since the magma left the mantle. Primitive lavas have equilibrium assemblages of phenocrysts and commonly have olivine or olivine + chromian spinel as their only phenocrysts. Olivine is typically Fo_{86-88} in tholeiitic (see below) and Fo_{86-90} in calc-alkaline lavas. The chromian spinel is present in a wide range of compositions that correlate with rock chemistry (Clynne & Borg 1997). Plagioclase phenocrysts (An_{70-90}) occur in some lavas, and clinopyroxene (typically diopside with 0.5–1.0% Cr_2O_3) also may be present, especially in basaltic andesite. Most samples in our data-set are comparatively rich in compatible trace elements (Fig. 2; *e.g.*, >140 ppm Ni, >200 ppm Cr), have high Mg contents (8–10.5 wt.% MgO), and a high Mg# [= 100Mg/(Mg + Fe^T)] (*i.e.*, >60). A few evolved samples were deliberately included in order to assess fractionation and contamination. Because primitive lavas are not common among the many monogenetic vents and shield volcanoes of any given center, detection of systematic across-arc compositional variation is hampered by the small number of samples; exploring larger data-sets of less primitive lavas is beyond the scope of this study (*cf.* Borg *et al.* 1997).

Many of the analyzed samples are poor in incompatible elements and belong to the group variously termed high-alumina basalt [HAB: Gerlach & Grove (1982); see Donnelly-Nolan *et al.* (1991, p. 21,856) for history of HAB terminology], high-alumina olivine tholeiite [HAOT: Hart *et al.* (1984), Bacon (1990), Barnes (1992)], or low-K olivine tholeiite (LKOT: Bullen & Clynne (1989); we will refer to these as HAOT. Other lavas are designated arc basalt ($SiO_2 \leq 52$ wt.%) or basaltic andesite ($SiO_2 > 52$ wt.%; a sample of magnesian andesite with 58 wt.% SiO_2 is included with basaltic andesite for simplicity). One sample in our set is an alkali basalt from the Simcoe volcanic field, east of Mount Adams in Washington; it represents a melt of intraplate-type mantle.

Our study addresses questions of mantle composition, influence of subduction, melting processes, and thermal structure in the mantle beneath the arc. Variation in the composition of the crust complicates interpretation of geochemical data, even for primitive lavas, as will be seen below. Nevertheless, by considering our new results, unpublished data, and the few published results of complete analyses of primitive rocks from elsewhere in the Cascades, we are able to suggest answers to these questions.

We used our knowledge of the eruptive histories and compositional variety of five volcanic centers that we have mapped in detail to guide us in choosing representative primitive lavas for analysis. It is important to appreciate that each of the five centers is a *volcanic field* with many vents, even though it may bear the name of a single large volcano (*e.g.*, Christiansen *et al.* 1977, Donnelly-Nolan 1988, Bacon 1990, Clynne 1990, Hildreth & Lanphere 1994). Although we attempted to characterize the primitive rocks of each center at the time this study was initiated, the entire

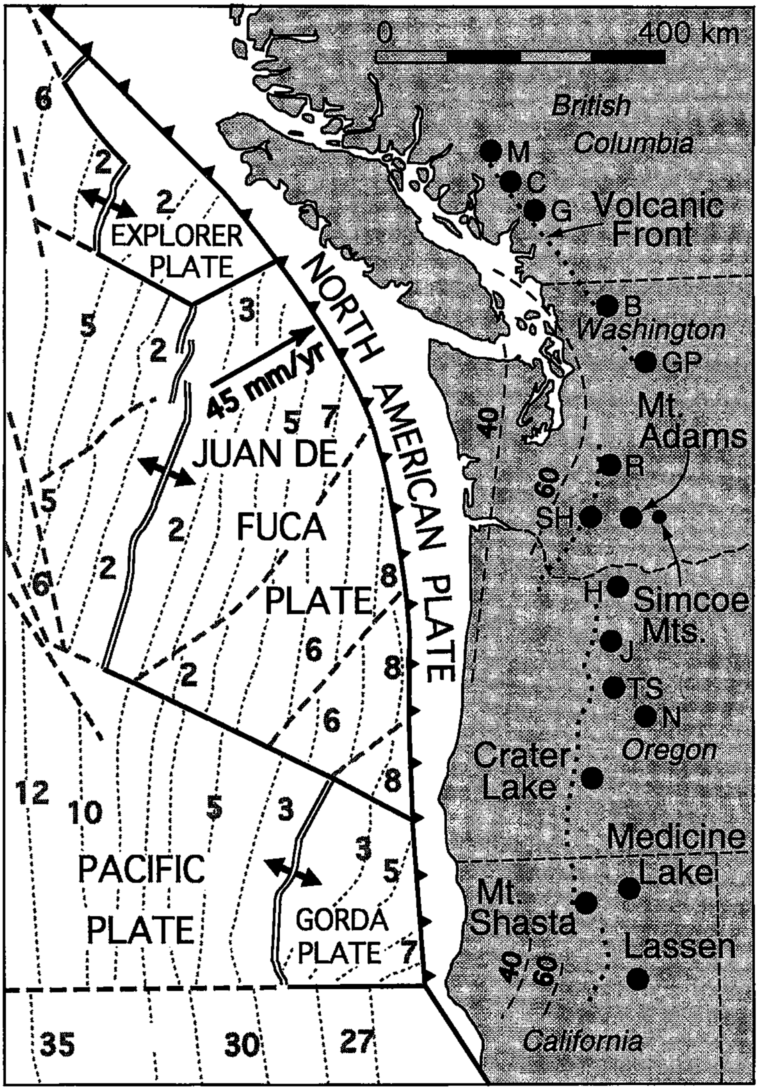

FIG. 1. Location map showing major Cascade volcanoes (dots), the Cascade volcanic front (short dashes), and plate tectonic features (modified after Muffler & Tamanyu 1995). Depth contours on the top of the slab (km) dashed where known. The number of the marine magnetic anomalies is shown for oceanic plates (age of anomaly 8 ≈ 11 Ma). The small, young Juan de Fuca and Gorda plates converge slowly with the North American Plate. Plate convergence is normal to the Cascade arc in northern Washington and British Columbia, oblique in southern Washington – northern California. The volcanic zone is ≥100 km wide at Mount Adams, Mount Shasta – Medicine Lake, and Lassen, ~30 km wide at Crater Lake. Volcanoes not part of this study: M, Meager Mountain; C, Mount Cayley; G, Mount Garibaldi; B, Mount Baker; GP, Glacier Peak; R, Mount Rainier; SH, Mount St. Helens; H, Mount Hood; J, Mount Jefferson; TS, Three Sisters; N, Newberry.

range of primitive compositions cannot be represented by a small number of samples, and our coverage of some centers is not comprehensive. In order to partially compensate for this inadequate coverage, our interpretations also consider published data and unpublished results of analyses in our files. Here, we report a new

TABLE 1. CHEMICAL AND ISOTOPIC ANALYSES OF PRIMITIVE LAVAS

Sample	MA-767	MA-696	MA-120	MA-953	MA-322	SM-27	75SH-270	75SV-3	75SH-317	75SH-268
Center	Mount Adams	Mount Adams	Mount Adams	Mount Adams	Mount Adams	Simcoe Mountains	Mount Shasta	Mount Shasta	Mount Shasta	Mount Shasta
Type*	HAOT	HAOT	HAOT	AB	AB	ALKB	HAOT	BA	BA	BA†
Latitude	46°03.64'	46°25.31'	46°19.31'	46°21.34'	46°02.14'	45°58.59'	41°14.58'	41°28.82'	41°21.93'	41°15.70'
Longitude	121°15.05'	121°45.41'	121°30.01'	121°42.68'	121°29.83'	120°57.29'	122°01.38'	122°11.39'	122°12.38'	122°13.14'
wt.%										
SiO_2	48.1	47.5	47.9	49.5	49.0	49.0	49.4	53.1	52.9	55.3
Al_2O_3	16.3	16.9	16.7	15.6	15.9	16.3	17.4	15.1	16.8	16.8
Fe_2O_3	1.77	1.96	1.5	2.41	3.07	4.66	1.21	3.21	2.15	1.55
FeO	9.30	9.31	9.27	6.40	5.92	6.25	8.00	4.15	5.20	5.11
MgO	9.62	8.85	8.78	9.62	8.87	6.28	9.30	9.78	8.94	6.59
CaO	10.1	10.5	10.25	9.81	9.40	7.33	10.9	9.73	9.62	8.75
Na_2O	2.85	2.85	3.02	3.17	3.50	4.17	2.68	2.99	3.06	3.35
K_2O	0.173	0.160	0.311	1.480	1.074	2.254	0.284	0.698	0.468	0.842
TiO_2	1.22	1.39	1.42	1.36	1.50	2.28	1.01	0.70	0.56	0.77
P_2O_5	0.11	0.16	0.16	0.52	0.39	0.9	0.11	0.21	0.11	0.18
MnO	0.17	0.18	0.18	0.14	0.14	0.15	0.17	0.13	0.13	0.11
H_2O+	0.31	0.30	0.20	0.16	0.22	0.50	0.21	0.44	0.22	0.28
H_2O-	0.13	0.11	0.07	0.07	0.11	0.16	0.09	0.23	0.10	0.18
CO_2	0.04	0.01	0.04	0.02	0.04	—	0.03	0.04	0.05	—
Total	100.19	100.18	99.80	100.26	99.13	100.23	100.79	100.51	100.31	99.81
Mg#	61.2	58.8	59.6	66.7	64.6	51.7	64.6	71.2	69.1	64.4
ppm										
Sc	28.8	32.9	32.7	28.0	25.9	13.8	36.3	27.4	27.2	23.2
V	189	217	212	180	208	147	220	201	198	184
Cr	345	275	300	347	326	129	389	500	476	226
Co	52.1	53.8	46.8	41.3	42.3	34.4	41.6	34.8	35.6	27.9
Ni	143	178	134	211	175	103	40	143	166	67
Cu	58	88	68	92	77	30	28	56	65	51
Zn	78	85	83	84	81	92	82	78	78	71
Rb	3.0	3.3	6.9	23.5	7.4	37.6	4.7	8.9	6.7	12.9
Cs	0.053	0.042	0.111	0.225	0.101	0.359	0.202	0.419	0.159	0.830
Sr	243	247	289	967	972	995	232	604	354	607
Ba	68	58	81	547	347	672	122	225	148	257
Pb	0.62	0.42	0.77	4.24	3.35	2.06	1.79	3.01	2.21	4.23
La	4.38	5.87	6.94	38.45	22.35	40.90	4.48	10.15	4.53	10.83
Ce	11.45	15.29	17.12	81.32	50.15	86.53	11.85	24.00	10.86	25.84
Nd	8.55	9.60	11.78	45.50	27.51	42.96	9.09	13.28	7.04	14.29
Sm	2.55	3.10	3.21	8.59	5.14	8.45	2.77	2.85	1.84	3.09
Eu	1.01	1.21	1.20	2.42	1.67	2.76	1.05	0.93	0.66	1.02
Gd	3.18	3.80	3.86	6.53	4.50	7.02	3.52	2.64	2.04	2.89
Dy	3.53	4.32	4.19	4.56	3.76	5.33	4.22	2.50	2.23	2.69
Er	2.03	2.59	2.60	2.64	2.11	2.42	2.68	1.45	1.37	1.53
Yb	1.79	2.39	2.20	1.90	1.74	1.93	2.50	1.34	1.30	1.38
Y	23	26	24	24	25	31	23	21	16	19
Zr	83	98	112	204	165	275	84	106	70	122
Hf	1.74	2.31	2.44	4.19	3.34	5.36	1.90	2.13	1.50	2.72
Nb	4.9	6.0	7.7	15	14	57	2.5	3.8	2.2	4.2
Ta	0.349	0.46	0.51	0.97	0.91	3.77	0.188	0.272	0.158	0.274
Th	0.59	0.62	0.68	5.09	2.33	3.96	0.64	1.74	0.76	2.56
U	—	—	—	—	0.78	1.31	—	0.60	—	0.90
$^{87}Sr/^{86}Sr$	0.70284	0.70292	0.70292	0.70360	0.70329	0.70306	0.70413	0.70366	0.70362	0.70344
$^{143}Nd/^{144}Nd$	0.512979	0.513013	0.513013	0.512925	0.512975	0.512874	0.512828	0.512899	0.512887	0.512875
$^{206}Pb/^{204}Pb$	19.037	18.925	18.856	18.967	18.872	18.692	18.803	18.865	18.776	18.842
$^{207}Pb/^{204}Pb$	15.567	15.568	15.540	15.583	15.559	15.525	15.611	15.587	15.569	15.595
$^{208}Pb/^{204}Pb$	38.528	38.475	38.359	38.630	38.473	38.283	38.541	38.491	38.384	38.509
$\delta^{18}O$	+5.7	+5.7	+5.7	+5.1	+5.5	+6.0	+6.7	+6.9	+6.7	+7.1

*HAOT, high-alumina olivine tholeiite; AB, arc basalt; BA, arc basaltic andesite; ALKB, alkali basalt.
†75SH-268 contains ~40 % phenocrysts of plagioclase + augite + orthopyroxene.
Analysts: D.F. Siems, major elements; S.T. Pribble, FeO, Na_2O, $H_2O\pm$, CO_2, Nb, V; T.L. Fries, K_2O; J.N. Grossman, Sc, Cr, Co, Zn, Cs, Hf, Ta, Th, U; O isotopes, L.H. Adami; rest, P.E. Bruggman. See text for methods.
Dash indicates that concentration was below detection limit or that element was not analyzed.

data-set that is internally consistent, precise (*e.g.*, concentrations of the rare-earth elements, *REE*, by isotope dilution), and reasonably complete in terms of the elements and isotopes of interest to geochemists.

Geological Setting

The Cascade volcanic arc extends from northern California to southern British Columbia (Fig. 1). Arc volcanism is associated here with subduction of the

TABLE 1. CHEMICAL AND ISOTOPIC ANALYSES OF PRIMITIVE LAVAS

Sample	81C621	82C894	84C1143	88C1540	88C1530	88C1521	88C1523	88C1557	80C354
Center	Crater Lake	Crater Lake	Crater Lake	Crater Lake	Crater Lake	Crater Lake	Crater Lake	Crater Lake	Crater Lake
Type	HAOT	HAOT	HAOT	HAOT	HAOT	BA	BA	BA	BA
Latitude	42°53.64'	42°56.04'	43°02.75'	43°02.74'	43°02.12'	43°00.87'	43°01.32'	43°04.65'	42°59.89'
Longitude	122°14.82'	122°25.27'	122°12.32'	122°12.15'	122°12.10'	122°10.17'	122°11.57'	122°09.48'	122°09.76'
wt.%									
SiO_2	47.5	47.4	48.7	48.9	49.9	53.8	52.2	52.1	53.0
Al_2O_3	17.4	17.3	17.0	17.2	17.2	16.3	16.0	17.3	16.7
Fe_2O_3	4.57	1.53	1.73	1.93	1.70	2.20	3.19	1.96	3.25
FeO	5.61	7.71	7.62	7.35	7.11	5.43	4.48	6.09	3.97
MgO	9.74	9.51	9.18	9.05	8.43	8.27	8.23	7.59	7.21
CaO	11.1	11.3	11.1	10.9	10.0	8.37	8.94	9.42	8.52
Na_2O	2.69	2.83	2.91	2.97	3.32	3.55	3.79	3.52	3.70
K_2O	0.107	0.083	0.255	0.333	0.522	0.882	1.122	0.669	1.216
TiO_2	1.08	1.04	1.17	1.16	1.18	0.96	1.14	1.12	1.03
P_2O_5	0.11	0.10	0.17	0.19	0.28	0.30	0.52	0.26	0.42
MnO	0.19	0.16	0.17	0.16	0.15	0.12	0.12	0.14	0.11
H_2O+	0.29	0.2	0.10	0.16	0.12	0.14	0.14	0.13	0.32
H_2O-	0.38	0.13	0.04	0.08	0.05	0.07	0.07	0.06	0.14
CO_2	0.04	—	—	—	—	—	—	—	0.02
Total	100.81	99.29	100.15	100.38	99.96	100.39	99.94	100.36	99.61
Mg#	64.1	65.1	64.1	64.0	63.5	66.6	66.6	63.3	65.1
ppm									
Sc	35.1	35.5	36.6	36.6	30.3	22.1	21.5	25.8	20.5
V	223	224	229	225	213	182	203	202	186
Cr	294	249	311	269	263	370	301	262	290
Co	48.7	47.5	44.7	44.9	39.0	36.5	33.0	35.5	33.2
Ni	196	174	149	138	123	167	163	107	161
Cu	82	105	101	84	82	73	37	66	68
Zn	72	72	80	75	73	79	85	73	84
Rb	1.0	—	2.5	5.7	6.7	13.4	13.6	6.5	13.4
Cs	0.048	0.040	0.052	0.082	0.092	0.258	0.173	0.208	0.435
Sr	310	295	381	421	580	744	1266	585	1347
Ba	72	46	112	136	224	334	485	259	571
Pb	0.58	0.49	1.00	1.31	1.17	2.95	3.35	2.64	5.21
La	2.61	2.35	5.02	6.13	10.53	13.81	27.48	9.93	23.12
Ce	9.17	7.61	14.68	18.72	27.67	32.10	57.36	24.62	50.28
Nd	8.45	7.36	11.19	12.67	16.49	17.02	27.63	13.39	25.08
Sm	2.72	2.43	3.15	3.27	3.77	3.51	4.81	3.55	4.47
Eu	1.08	0.97	1.14	1.15	1.29	1.09	1.43	1.24	1.35
Gd	3.50	3.14	3.45	3.74	3.96	3.22	3.69	3.63	3.51
Dy	4.08	3.69	4.19	4.26	4.05	2.89	2.83	3.60	2.75
Er	2.52	2.29	2.60	2.59	2.44	1.59	1.51	2.07	1.45
Yb	2.31	2.07	2.36	2.44	2.28	1.42	1.27	1.85	1.25
Y	21	20	23	21	21	16	15	21	19
Zr	76	69	100	105	125	120	150	130	158
Hf	1.86	1.67	2.21	2.42	2.75	2.67	2.99	2.81	3.23
Nb	1.3	1.3	2.4	2.6	3.5	4.9	6.8	4.1	6.9
Ta	—	0.13	0.174	0.201	0.256	0.321	0.51	0.27	0.408
Th	0.37	—	0.63	0.89	1.40	2.10	3.24	1.19	2.76
U	—	—	—	0.32	0.45	0.51	0.81	0.52	0.87
$^{87}Sr/^{86}Sr$	0.7035	0.70346	0.70355	0.70355	0.70361	0.70363	0.70375	0.70349	0.70372
$^{143}Nd/^{144}Nd$	0.512902	0.512953	0.512899	0.512893	0.512931	0.512895	0.512896	0.512942	0.512905
$^{206}Pb/^{204}Pb$	18.885	18.852	18.909	18.899	18.924	18.877	18.898	18.842	18.870
$^{207}Pb/^{204}Pb$	15.573	15.568	15.582	15.569	15.602	15.571	15.568	15.553	15.564
$^{208}Pb/^{204}Pb$	38.481	38.437	38.518	38.490	38.565	38.469	38.485	38.385	38.429
$\delta^{18}O$	+5.7	+6.0	+5.8	+5.9	+6.3	+6.4	+6.5	+6.5	+5.8

young Juan de Fuca and Gorda plates. From Glacier Peak northward, convergence is normal to the axis of the arc, and volcanism is restricted to comparatively isolated composite volcanoes and dome clusters (Rogers 1985, Guffanti & Weaver 1988). Between Mount Adams and the Lassen volcanic center, subduction is oblique, and the arc consists of widely spaced major composite volcanoes and abundant monogenetic volcanoes ranging from cinder cones to shields. There is no consensus as to whether features such as the Medicine Lake shield volcano, which lies behind the main axis of the arc, should be considered "Cascade" volcanoes. We include them in the scope of this paper in order to obtain a complete picture of magmatism in the Cascade arc.

TABLE 1. CHEMICAL AND ISOTOPIC ANALYSES OF PRIMITIVE LAVAS

Sample	LC88-1398	LC86-1046	LC82-970	LC88-1311	LC86-1005	LM87-1384	LC88-1312	LC82-905	LC86-855	LC85-671
Center	Lassen	Lassen	Lassen	Lassen	Lassen	Lassen	Lassen	Lassen	Lassen	Lassen
Type	AB	HAOT	HAOT	HAOT	AB	AB	AB	AB	AB	AB
Latitude	40°00.90'	40°26.47'	40°23.44'	40°19.20'	40°40.12'	40°32.16'	40°20.46'	40°32.47'	40°31.88'	40°38.75'
Longitude	121°57.77'	121°59.15'	121°17.51'	122°03.94'	121°45.06'	121°11.78'	122°03.08'	121°09.20'	121°02.93'	121°09.83'
wt.%										
SiO_2	49.5	48.2	48.4	48.0	51.3	49.8	50.8	49.7	49.5	51.0
Al_2O_3	16.4	17.4	17.4	18.0	15.7	15.6	16.6	17.5	16.7	16.9
Fe_2O_3	1.78	1.81	1.68	2.35	1.7	3.24	1.22	2.33	3.66	2.64
FeO	7.40	7.46	7.76	6.63	6.36	5.39	6.48	6.22	5.80	6.02
MgO	10.3	10.1	9.79	9.34	11.1	10.7	9.97	8.32	8.19	8.00
CaO	10.5	11.4	11.2	11.2	10.7	9.81	11.0	9.66	9.79	9.08
Na_2O	2.41	2.55	2.68	2.52	2.45	3.06	2.48	3.10	3.25	3.12
K_2O	0.403	0.138	0.172	0.157	0.317	0.924	0.299	0.659	0.830	1.006
TiO_2	0.85	0.80	0.96	0.81	0.52	1.32	0.73	0.98	1.34	1.18
P_2O_5	0.11	0.09	0.10	0.09	0.08	0.46	0.10	0.25	0.28	0.30
MnO	0.17	0.17	0.17	0.16	0.14	0.15	0.15	0.16	0.15	0.15
H_2O+	0.49	0.11	0.13	0.48	0.13	0.16	0.18	0.38	0.2	0.42
H_2O-	0.22	0.05	0.05	0.37	0.05	0.04	0.05	0.36	0.13	0.02
CO_2	0.07	0.02	0.03	0.05	—	0.04	—	—	0.04	0.04
Total	100.60	100.30	100.52	100.16	100.55	100.69	100.06	99.62	99.86	99.88
Mg#	67.1	66.5	65.3	65.6	71.5	69.7	70.1	64.1	61.6	62.9
ppm										
Sc	38.1	40.0	43.0	40.1	34.0	26.3	37.6	32.4	28.7	25.0
V	215	218	228	227	228	249	214	218	237	206
Cr	402	229	323	235	628	448	501	323	249	317
Co	43.9	46.1	48.1	45.0	43.7	40.0	38.5	38.5	38.1	36.7
Ni	213	190	184	180	209	152	85	144	117	155
Cu	79	93	121	94	69	50	32	74	66	71
Zn	70	70	74	71	68	91	70	81	85	77
Rb	6.2	—	3.5	1.3	3.3	16.1	4.7	7.2	10.9	16.3
Cs	0.319	0.032	0.062	0.057	0.107	0.295	0.226	0.229	0.265	0.402
Sr	237	241	235	245	294	601	520	405	449	486
Ba	268	76	89	85	112	413	108	276	343	360
Pb	2.32	1.02	1.20	1.00	1.40	3.90	1.40	4.30	3.03	3.31
La	7.94	3.03	4.44	4.00	3.69	20.76	6.99	11.48	13.02	13.47
Ce	17.93	8.43	9.94	8.81	8.96	49.60	16.44	26.52	31.75	31.18
Nd	10.69	6.91	8.03	7.14	6.09	26.45	9.48	14.87	18.46	17.44
Sm	2.78	2.17	2.57	2.23	1.69	5.20	2.26	3.35	4.28	3.93
Eu	0.96	0.87	1.00	0.88	0.61	1.47	0.83	1.05	1.36	1.30
Gd	3.21	2.95	3.44	3.03	1.98	4.20	2.58	3.32	4.36	3.99
Dy	3.92	3.95	4.42	3.88	2.22	3.27	3.20	3.46	4.18	3.85
Er	2.60	2.74	2.97	2.67	1.45	1.71	2.21	2.14	2.41	2.22
Yb	2.58	2.80	2.95	2.69	1.44	1.50	2.20	2.02	2.21	2.06
Y	21	19	24	21	14	16	19	19	21	18
Zr	76	60	79	64	59	142	80	108	121	129
Hf	1.74	1.38	1.79	1.47	1.14	3.10	1.72	2.43	2.68	2.7
Nb	2.0	1.5	2.1	1.8	1.5	11	2.2	7.8	7.3	9.3
Ta	0.15	—	0.16	0.12	—	0.691	0.162	0.511	0.498	0.63
Th	2.50	0.27	0.45	0.32	0.61	2.34	0.68	1.74	1.75	1.93
U	0.61	—	—	—	0.41	0.62	—	0.58	0.73	0.31
$^{87}Sr/^{86}Sr$	0.70420	0.70380	0.70381	0.70379	0.70383	0.70408	0.70317	0.70389	0.70400	0.70392
$^{143}Nd/^{144}Nd$	0.512770	0.512875	0.512891	0.512905	0.512898	0.512828	0.512970	0.512833	0.512800	0.512780
$^{206}Pb/^{204}Pb$	18.715	18.751	18.952	18.947	18.863	18.835	18.814	19.012	18.838	18.858
$^{207}Pb/^{204}Pb$	15.601	15.581	15.593	15.589	15.608	15.599	15.579	15.621	15.605	15.602
$^{208}Pb/^{204}Pb$	38.438	38.398	38.556	38.558	38.506	38.512	38.388	38.677	38.526	38.523
$\delta^{18}O$	+7.2	+6.1	+5.8	+6.7	+5.6	+6.9	+6.9	+5.9	+6.8	+7.4

Chemically primitive lavas are present throughout most of the arc in the zone of oblique convergence. These typically issued from monogenetic cinder cones, shields, or fissure vents.

From the Three Sisters to Lassen, the Basin and Range province impinges upon the arc, so that NW–SE to N–S normal faults are common at least as far west as the arc axis. Normal faults in the Cascades continue as far north as the Columbia River (Walker & MacLeod 1991), but do not occur in southern Washington. Pre-Cenozoic crystalline basement of the sub-arc crust is widely exposed north of a point approximately midway between Mounts Adams and Rainier. From Mount Shasta to the south, Mesozoic and Paleozoic oceanic and immature continental terranes are exposed adjacent to the arc. The intervening region, however, lacks basement exposures, and the modern arc is constructed on Tertiary arc volcanic rocks. Tertiary plutons cut these and basement rocks in the north, and locally as far south as central Oregon. There may be no pre-Tertiary base-

TABLE 1. CHEMICAL AND ISOTOPIC ANALYSES OF PRIMITIVE LAVAS

Sample	LC86-1009	82-72-f	767M	880M	1085M	851M	1376M	881M	1161M
Center	Lassen	Medicine Lake	Medicine Lake	Medicine Lake	Medicine Lake	Medicine Lake	Medicine Lake	Medicine Lake	Medicine Lake
Type	BA	HAOT	HAOT	HAOT	HAOT	HAOT	HAOT	HAOT	HAOT
Latitude	40°44.03'	41°30.3"	41°47.1"	41°30.0"	41°54.5"	41°47.2"	41°32.9"	41°30.0"	41°30.7"
Longitude	121°50.13'	121°38.7"	121°36.9"	121°37.9"	121°38.6"	121°34.0"	121°14.1"	121°38.0"	121°37.5"
wt.%									
SiO_2	58.2	47.6	47.3	47.9	48.0	47.6	47.9	49.0	52.7
Al_2O_3	16.0	18.5	18.0	18.3	17.8	18.4	18.2	17.7	16.7
Fe_2O_3	1.66	2.06	1.5	1.24	1.94	1.75	1.83	1.17	1.34
FeO	4.13	6.33	7.2	7.31	7.15	7.10	7.29	7.86	6.90
MgO	7.57	10.5	10.4	10.3	10.3	9.91	9.40	8.63	6.85
CaO	7.72	12.0	11.8	12.1	11.9	11.7	11.3	11.4	9.55
Na_2O	3.48	2.26	2.38	2.33	2.43	2.47	2.46	2.78	3.05
K_2O	0.806	0.074	0.062	0.073	0.085	0.094	0.114	0.333	1.092
TiO_2	0.52	0.59	0.71	0.63	0.74	0.77	0.80	0.90	0.92
P_2O_5	0.12	0.06	0.08	0.05	0.08	0.10	0.07	0.11	0.13
MnO	0.10	0.15	0.15	0.15	0.16	0.16	0.16	0.16	0.15
H_2O+	0.21	0.19	0.23	0.26	0.17	0.23	0.70	0.17	0.35
H_2O-	0.09	0.09	0.14	0.13	0.14	0.10	0.38	0.06	0.20
CO_2	—	0.17	0.20	0.03	0.02	0.05	—	0.02	0.02
Total	100.61	100.57	100.15	100.80	100.92	100.43	100.60	100.29	99.95
Mg#	70.6	69.6	68.4	68.6	67.4	67.1	65.2	63.3	60.1
ppm									
Sc	19.2	31.8	35.8	34.8	37.8	35.7	40.8	35.5	32.0
V	149	178	184	182	196	192	202	205	191
Cr	242	176	225	189	227	201	213	158	127
Co	29.5	48.6	50.1	49.7	50.7	48.6	47.3	43.9	37.1
Ni	171	218	207	205	185	176	164	123	104
Cu	50	126	105	118	74	111	110	117	102
Zn	61	55	63	58	60	65	65	76	64
Rb	10.9	1.5	—	—	2	1	—	11.9	31.4
Cs	0.429	0.078	0.022	0.080	0.029	—	0.028	0.491	2.04
Sr	762	178	211	177	211	224	255	199	193
Ba	179	17	48	29	40	47	79	87	249
Pb	3.40	—	0.35	0.35	0.31	0.38	0.61	1.13	3.21
La	7.53	1.25	1.66	1.33	1.98	1.81	2.65	3.87	8.08
Ce	16.04	3.82	4.82	4.04	5.01	5.47	6.35	10.37	19.20
Nd	9.32	3.62	4.79	3.83	5.17	5.23	5.74	7.76	11.38
Sm	2.12	1.34	1.68	1.42	1.75	1.81	1.90	2.42	3.06
Eu	0.73	0.62	0.73	0.65	0.74	0.78	0.83	0.94	1.01
Gd	2.01	1.96	2.37	2.10	2.46	2.50	2.65	3.20	3.64
Dy	1.85	2.66	3.15	2.85	3.16	3.26	3.47	4.00	4.46
Er	1.06	1.76	2.10	1.89	2.08	2.17	2.30	2.60	2.88
Yb	0.98	1.70	2.06	1.83	1.99	2.07	2.19	2.50	2.86
Y	13	15	19	22	23	19	27	27	31
Zr	92	46	56	51	61	54	68	94	135
Hf	1.83	1.01	1.18	0.96	1.21	1.23	1.41	1.89	3.02
Nb	2.6	1.1	—	1.2	1.0	—	1.3	1.8	3.2
Ta	0.155	0.11	—	—	—	—	0.11	0.20	0.38
Th	1.14	—	0.27	0.28	—	0.19	0.36	1.03	4.17
U	0.80	—	—	—	—	—	—		1.53
$^{87}Sr/^{86}Sr$	0.70305	0.70344	0.70344	0.70344	0.70342	0.70344	0.70358	0.70341	0.70346
$^{143}Nd/^{144}Nd$	0.512869	0.512968	0.512965	0.512932	0.512936	0.512974	0.512936	0.512950	0.512932
$^{206}Pb/^{204}Pb$	18.674	18.692	18.873	18.819	18.914	18.872	18.881	18.831	18.911
$^{207}Pb/^{204}Pb$	15.535	15.627	15.569	15.576	15.573	15.565	15.590	15.538	15.582
$^{208}Pb/^{204}Pb$	38.217	38.406	38.468	38.446	38.463	38.420	38.536	38.387	38.528
$\delta^{18}O$	+6.9	+5.9	+5.8	+5.8	+5.9	+5.7	+6.3	+5.2	+5.9

ment beneath the Cascade arc between Mount Adams and ~100 km north of Crater Lake (Riddihough *et al.* 1986). Here, beneath the arc, the basement is likely to be composed of accreted Early Tertiary oceanic basalt and marine sedimentary rocks (*e.g.*, Wells & Heller 1988, Trehu *et al.* 1994).

The continental crust is ~40 km thick beneath the Mount Adams volcanic field (Mooney & Weaver 1989). A reversed seismic refraction profile ~30 km west-southwest of Crater Lake defined a crustal thickness of 44 km (Leaver *et al.* 1984), although it is uncertain if this is the case under the volcanic field. Extensive seismic refraction surveys of the Mount Shasta – Medicine Lake area delineate crustal structure but not total thickness (Fuis *et al.* 1987), which Mooney & Weaver suggested is 38–40 km. Crustal thickness beneath the Lassen region is 38 ± 4 km (Mooney & Weaver 1989).

METHODS

Samples

Samples were selected from collections made during geological mapping of Mount Adams (Hildreth & Fierstein 1995), Mount Mazama and Crater Lake caldera (Bacon, unpubl. map, 1995), Mount Shasta (Christiansen, unpubl. map, 1995), the Medicine Lake volcano (Donnelly-Nolan, unpubl. map, 1995), and the Lassen volcanic center (Clynne & Muffler, unpubl. map, 1995). Powders were ground in an alumina shatterbox. Although many samples had been analyzed previously, the entire set was re-analyzed as a group (except for isotopic compositions and some *REE* abundances) in order to improve precision.

Major elements

Major elements were determined by wavelength-dispersion X-ray fluorescence (XRF) on fused glass disks in Lakewood, Colorado. The Na_2O and K_2O values given in Table 1 were determined by flame photometry. Ferrous iron, $H_2O^{\pm}$, and CO_2 contents were determined by standard wet-chemical methods.

Trace elements

Lead and *REE* concentrations were measured by isotope-dilution mass spectrometry. Energy-dispersion XRF was used for Rb, Sr, Y, Zr, Ba, Ni, and Cu concentrations. Concentrations of Nb and V were determined by inductively coupled plasma – atomic emission spectrometry (ICP–AES) following quantitative chemical separation. Although the Nb values are precise, there is some question as to their accuracy at the lowest concentrations reported because of poor knowledge of concentrations in standards. The concentrations of the remaining elements reported in Table 1 (Cs, Sc, Cr, Co, Zn, Hf, Ta, Th, and U) were measured by instrumental neutron-activation analysis (INAA) in Reston, Virginia. In a few samples, some of these elements are present at concentrations below detection limits. A special effort was made to obtain data for Cs by INAA by counting after approximately one year in order to allow interfering nuclides to decay to low levels.

Isotopes

Isotopic compositions of Sr, Nd, Pb, and O (Table 1) were determined for all 38 samples of this study. Analyses (Sr, Nd, Pb) were performed with a Finnigan MAT 262 variable multicollector mass spectrometer. Measured $^{86}Sr/^{88}Sr$ ratios were normalized to a value of 0.1194, and $^{146}Nd/^{144}Nd$ ratios, to a value of 0.7219. Empirical thermal mass-fractionation corrections of 0.11‰ per mass unit were applied to Pb isotope measurements. Oxygen was extracted with ClF_3, converted to CO_2, and analyzed using a modified Nier-type, 6-inch dual-collecting mass spectrometer. Reported whole-rock $\delta^{18}O$ values are calibrated to a $\delta^{18}O$ value of +9.6‰ for NBS–28 quartz relative to the SMOW standard. Further details of analytical procedures for isotopic compositions are given in Bacon *et al.* (1994).

PRIMITIVE MAGMA-TYPES

We recognize three *end-member* primitive magma-groups in the Cascades, characterized mainly by their trace-element and alkali-metal abundances: high-alumina olivine tholeiite, arc basalt and basaltic andesite, and intraplate basalt. Names of these end-members reflect historical precedent, the subduction-related geochemistry of "arc" basalt and basaltic andesite, and the fact that tholeiitic and intraplate basalts are not limited in occurrence to the arc itself. We emphasize that a continuum of compositions seems to exist between these end-members, although examples intermediate between extreme-arc and intraplate varieties are scarce, and that assignment of some lavas with intermediate characteristics to any one group is somewhat arbitrary.

A fundamental observation is that approximately coeval lavas of different types have erupted from nearby vents. A corollary is that Quaternary across-arc compositional variation, present where the volcanic arc is wide, is manifested only in the broadest terms by occurrence of extreme subduction-component-enriched magmas in the fore-arc and more alkaline, intraplate types in the back-arc region (*e.g.*, Lassen area; Borg *et al.* 1997).

High-alumina olivine tholeiite (HAOT)

Primitive HAOT occurs locally throughout the Cascades from southern Washington to northern California. The field occurrence of HAOT reflects the low viscosity of these normally phenocryst-poor to aphyric magmas. Vents are marked by low shield summits, pit craters, small spatter cones, or spatter ramparts along eruptive fissures. Pahoehoe flow surfaces are common in complex sequences of many related flows, each of which may be as little as 0.5 m thick, but in their entirety may total many tens of meters in intracanyon settings or topographic depressions. Tube-fed HAOT flow fields, such as the Giant Crater flows at Medicine Lake (Donnelly-Nolan *et al.* 1991), extend as much as 45 km from their vents. Diktytaxitic texture and subophitic groundmass augite are common in HAOT.

The major-element compositions of HAOT samples are similar to those of mid-ocean ridge basalt, MORB,

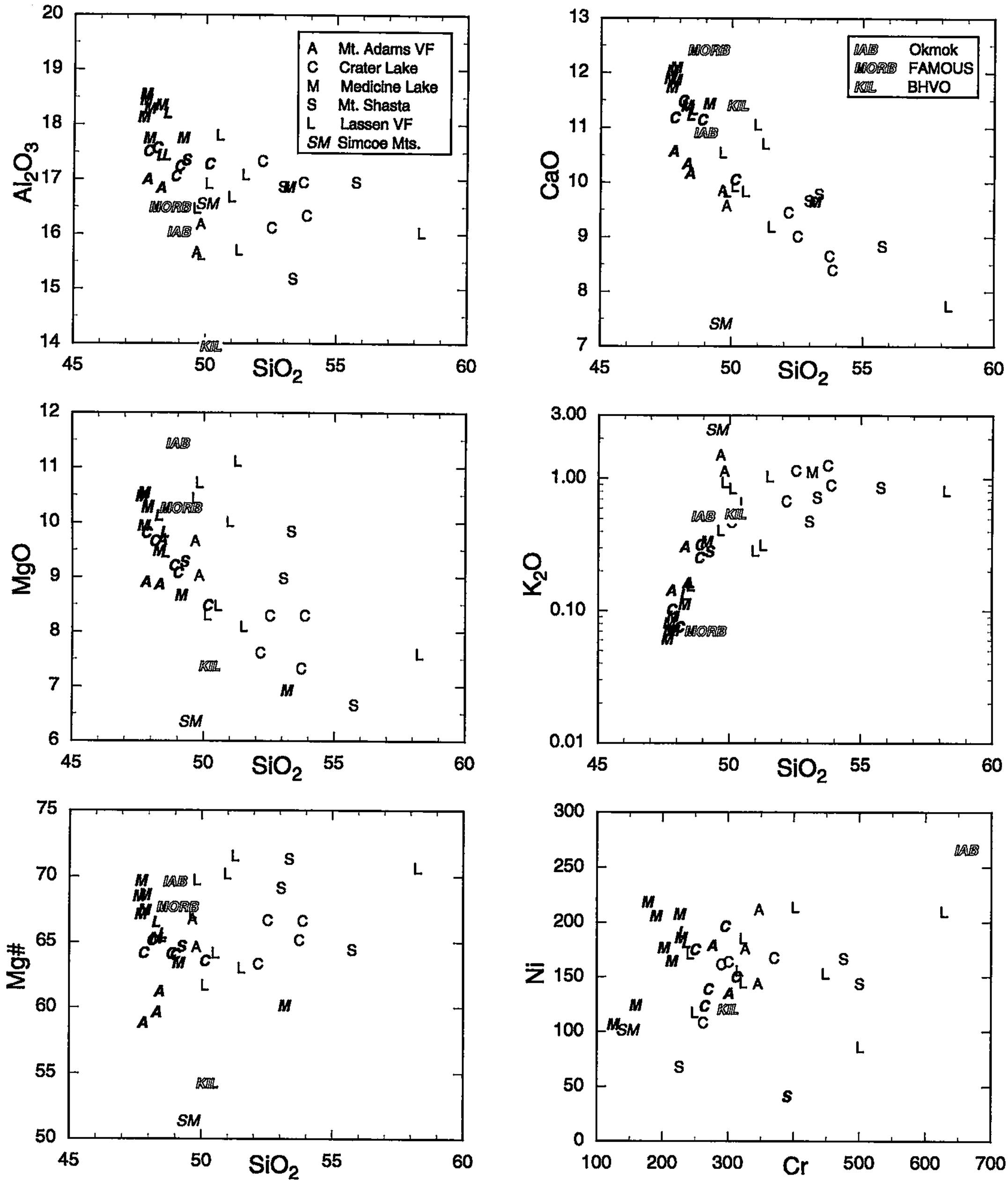

FIG. 2. Selected variation diagrams (major-element oxides recalculated to sum to 100 wt.% volatile-free and with all Fe as FeO*, Ni and Cr in ppm). Bold italic letters identify samples of HAOT, including differentiated and contaminated sample from Medicine Lake. Note log scale for K_2O in order to show variation in HAOT. Non-italic letters identify arc basalt and basaltic andesite, which have higher SiO_2, K_2O, and Cr, generally lower Al_2O_3 and CaO contents than HAOT; MgO and Mg# [100MgO/(MgO + FeO*), molar] can be comparable. *SM* is mantle-xenolith-bearing alkali basalt from the Simcoe Mountains volcanic field. High Ni content and Mg# of most samples, including basaltic andesites, imply that they are primitive. Representative basalts in this and other figures plotted for reference: *IAB* is Okmok basalt sample ID–16 of Nye & Reid (1986), *KIL* is Kilauea basalt standard *BHVO* (Abbey 1983), and *MORB* is a FAMOUS area mid-ocean ridge basalt (Langmuir *et al.* 1977).

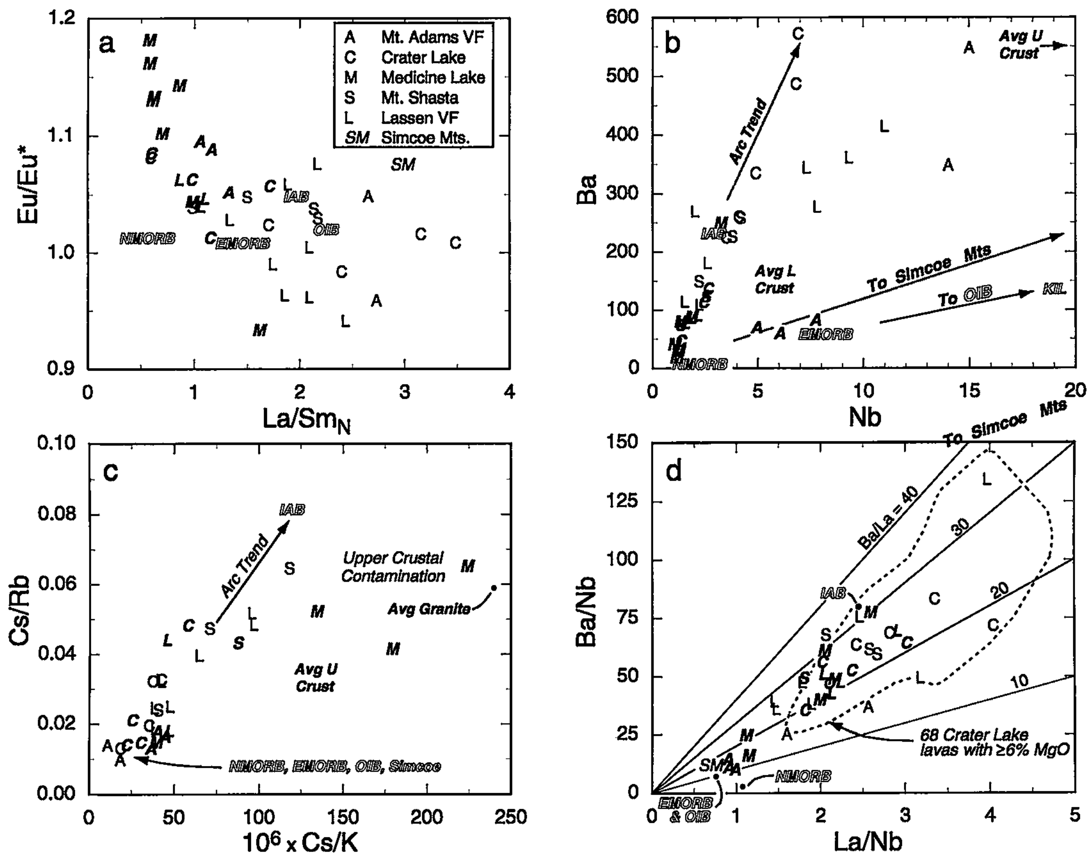

FIG. 3. Characteristic trace-element ratios and concentrations. In this and subsequent diagrams, *N-MORB*, *E-MORB*, and *OIB* are from Sun & McDonough (1989). a) Chondrite-normalized (Sun & McDonough 1989) La/Sm *versus* Eu/Eu*. b) Nb *versus* Ba concentrations (ppm). Trend "To Simcoe Mountains" refers to sample labeled *SM* in other figures (672 ppm Ba, 57 ppm Nb). Most samples plot along the arc trend, but those from the Mount Adams and four from the Lassen volcanic fields are richer in Nb at comparable Ba contents. Average upper and lower crust (*Avg U Crust, Avg L Crust*) are from Taylor & McLennan (1995). c) Cs–Rb–K relations. Coupled Cs/Rb and Cs/K ratios higher than in oceanic basalts reflect modern subduction-derived component in arc basalt and basaltic andesite, ancient(?) in HAOT-source. "Upper crustal contamination" refers to Giant Crater lavas, shown by Baker *et al.* (1991) to have assimilated hypabyssal granite (three Medicine Lake samples with high Cs/K ratios). *Avg Granite* is the average of 8 granitic xenoliths in the Burnt Lava flow at Medicine Lake (Grove *et al.* 1988). d) La/Nb *versus* Ba/Nb ratios showing lines of equal Ba/La ratio. Higher Ba/Nb ratios than *N-MORB* at La/Nb > 1 for all samples except three from Mount Adams and the Simcoe Mountains alkali basalt reflect presence of a subduction-derived component. The low Ba/La value of Mount Adams samples is in keeping with a relatively strong intraplate geochemical signature there. Field for lavas from Crater Lake area with ≥6% MgO from Bruggman *et al.* (1989) and C.R. Bacon (unpubl. data, 1995).

but are distinguished by higher Al contents, commonly >17% Al_2O_3 (Fig. 2). In comparison to other primitive Cascade lavas, HAOTs have high Ca (most >11% CaO; Fig. 2) and low Na (~2.5% *versus* ≥3% Na_2O). Incompatible elements are present at concentrations nearly as low as, or similar to, those in MORB, as exemplified by K (commonly <0.10% K_2O: Fig. 2). Measurements of dissolved H_2O in melt inclusions in olivine from Medicine Lake suggest that HAOT magmas had pre-eruptive H_2O contents of ≤0.3% (Sisson & Layne 1993). Concentrations of Ba, Cs, Rb, Th, Sr, and Pb, however, are typically higher in HAOT than in N–MORB. Some HOAT samples have Cs/K and Cs/Rb ratios notably higher than values typical of OIB, ocean-island basalt, or MORB, and they plot along the arc trend in Figure 3c. Likewise, HAOT samples have high

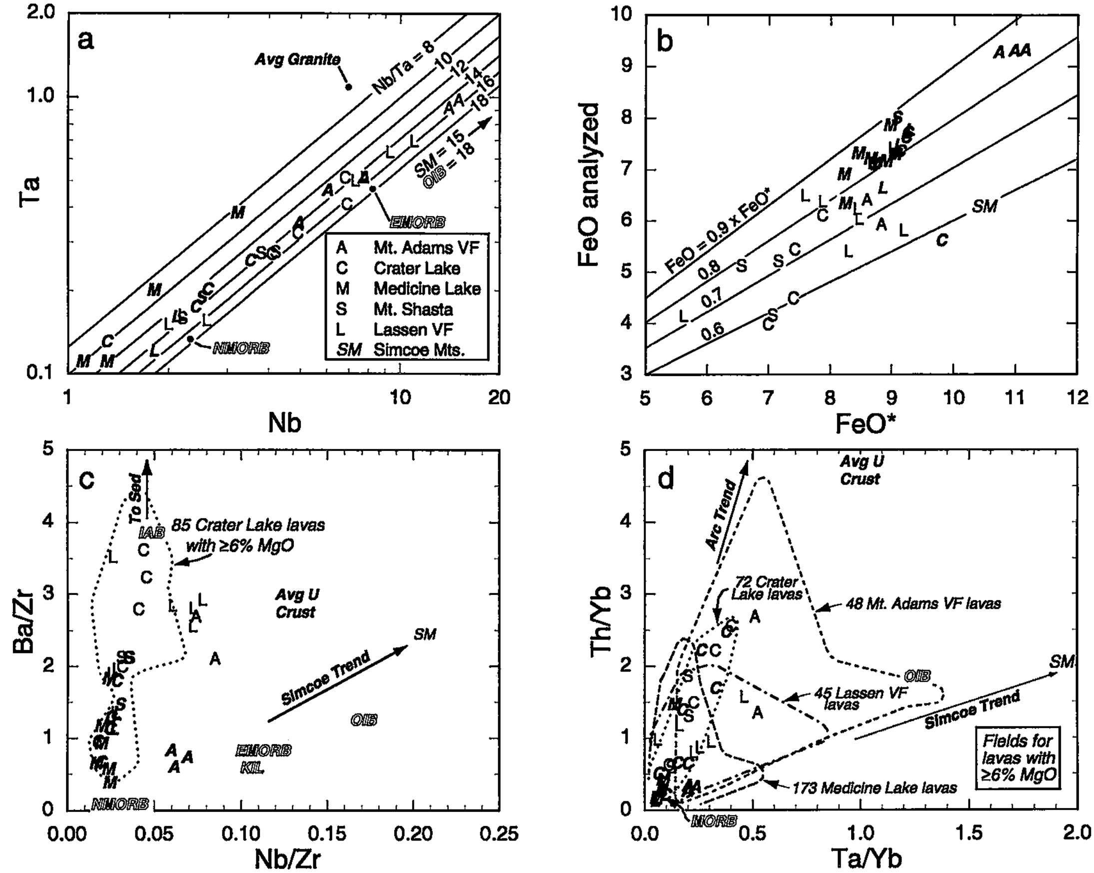

FIG. 4. Concentrations of Nb and Ta, FeO–FeO* relations, and element-ratio discrimination diagrams. a) Nb *versus* Ta (ppm), showing lines of equal Nb/Ta ratio. Most samples have Nb/Ta ratios lower than oceanic basalts. Precision is poor at low abundances, so Nb/Ta ratios for samples with Nb < 2 ppm are imprecise. Two Medicine Lake samples with Nb/Ta ≈ 9 are HAOT fractionates contaminated with hypabyssal granite represented by *Avg Granite*, the average composition of 8 xenoliths in the Burnt Lava flow at Medicine Lake (Grove *et al.* 1988). b) Analyzed FeO contents *versus* total Fe as FeO* showing lines of equal FeO/FeO* ratio. Arc basalts and basaltic andesites typically are more oxidized than samples of HAOT. c) Nb/Zr *versus* Ba/Zr ratios (after Leeman *et al.* 1990, Figure 7b). This diagram separates intraplate (high Nb/Zr) from subduction-related (high Ba/Zr) magmas. Evidence for an intraplate component in the present data-set exists for Lassen and Mount Adams volcanic fields (compare with Fig. 4d). Dotted field encloses compositions of 85 lavas from the Crater Lake area with ≥6% MgO (Bruggman *et al.* 1989; C.R. Bacon, unpubl. data, 1995). Average upper crust (*Avg U Crust*) is from Taylor & McLennan (1995), and probably has higher Nb/Zr and Ta/Yb than Cascade arc crust. Pelagic sediment composition (*To Sed*) is from Hole *et al.* (1984). d) Ta/Yb *versus* Th/Yb ratios. Expanded data-sets for all but the Shasta area show presence of a high-(Ta/Yb) intraplate component at Mount Adams, Lassen, and Medicine Lake volcanic fields, but not at Crater Lake. Field for lavas from Crater Lake area as in Figure 4c. Fields for Mount Adams, Lassen, and Medicine Lake volcanic fields from unpublished data of W. Hildreth, M.A. Clynne, and J.M. Donnelly-Nolan, respectively (1995). *MORB* in this figure represents both N-MORB and E-MORB of Sun & McDonough (1989).

Ba/Nb, Ba/La, and La/Nb ratios (many have La/Nb > 2), except for those from the Mount Adams volcanic field (Fig. 3d). This subduction-related signature also is present in HAOT from east of the Cascades (Hart *et al.* 1984; W.K. Hart, unpubl. data, 1995), suggesting that enrichment of the large-ion lithophile elements, *LILE*, in HAOT is not related to modern subduction and the present Cascade arc, but is an older subduction-related feature that is characteristic of the HAOT source over a larger region.

The lavas from Medicine Lake are the most incompatible-element-depleted in this study. They include primitive through moderately differentiated and contaminated lavas, in part from the Giant Crater lava field (Donnelly-Nolan *et al.* 1991). The distinct trend of the Medicine Lake samples toward high Cs/K (Fig. 3c) reflects assimilation of granite, as documented in the Burnt Lava (Grove *et al.* 1988), the Giant Crater flows (Baker *et al.* 1991), and Lake Basalt (Wagner *et al.* 1995).

Chondrite-normalized *REE* patterns for HAOT are *LREE*-depleted to slightly *LREE*-enriched. Heavy *REE* concentrations are generally ≥10 × chondrites, considerably higher than in most primitive arc basalts and basaltic andesites of the Cascades. Positive Eu anomalies (Eu/Eu* up to ~1.2) are negatively correlated with La/Sm_N (Fig. 3a).

The Nb/Ta ratio varies significantly among our HAOT samples (Fig. 4a). Most have Nb/Ta ratios of ~12–16, significantly lower than MORB, OIB, or chondritic values of 17–18 given by Sun & McDonough (1989). There is a tendency for increasing Nb/Ta with increasing abundances of these elements in the Cascade lavas, although this is somewhat equivocal because of potential systematic error at low concentrations. These observations are not readily explained by a single-stage partial melting process because the ratio of crystal/melt partition coefficients, D^{Nb}/D^{Ta}, is generally ≤1 for virtually all phases that have been studied experimentally (Green 1995). Plank & White (1995) suggested that the cause of sub-chondritic Nb/Ta values they measured for low-(Nb,Ta) arc basalts and MORB may be source depletion by prior extraction of low-degree, relatively high-(Nb/Ta) partial melt. Judging from the compositions of granitic xenoliths presented by Grove *et al.* (1988), the two Medicine Lake samples with Nb/Ta ratios of ~9 have these low values, and relatively high Nb and Ta concentrations, because of assimilation of granite, as described by Baker *et al.* (1991).

Compatible trace-element abundances are somewhat diagnostic of magma type. Although both HAOT and arc lavas have Ni concentrations up to ~200 ppm, Cr values in HAOT lavas do not exceed ~400 ppm (Fig. 2). HAOT lavas typically have higher Co and Sc concentrations (most >40 and >30 ppm, respectively) than the arc lavas.

Arc basalt and basaltic andesite

Arc ("calc-alkaline") basalt and basaltic andesite lavas are abundant near the axis of the Quaternary Cascades as far north as southern Washington. They commonly have more abundant olivine and plagioclase phenocrysts than HAOT, and may also contain clinopyroxene; some lack plagioclase phenocrysts. Higher SiO_2 content and probable lower temperatures of eruption translate to higher viscosities and a different mode of occurrence. These magmas erupted from vents marked by cinder cones or form cone-capped shields. The flows themselves are thicker and, where preserved, have blocky or aa surfaces.

Primitive arc basalts and magnesian basaltic andesites have higher SiO_2 contents and comparable or even higher Mg# than found in HAOT (Fig. 2). Most do not reach the extreme CaO and MgO contents of HAOT [Fig. 2; note, however, that some compositions given in Clynne (1993) and Baker *et al.* (1994) have MgO as high as in HAOT]. Arc basalt and basaltic andesite are characterized by the *LILE* (Cs, Rb, K, Ba, Sr, Pb, Th, U) enrichment relative to the *HFSE* (Nb, Ta, Zr, Hf, Ti) typical of arc magmas, and greater than that in HAOT as seen, for example, in a plot of Nb *versus* Ba (Fig. 3b). Cs/K and Cs/Rb ratios (Fig. 3c) are higher than MORB or OIB values (Morris & Hart 1983, Ben Othman *et al.* 1989), as noted above for some HAOT samples, and trend toward primitive Aleutian arc basalt (Nye & Reid 1986).

Light *REE* enrichment relative to *HREE* and *HFSE* is typical of Cascade primitive arc basalt and basaltic andesite. In these rocks, La/Nb ratios range from 1.5 to 4, far higher than in MORB or intraplate basalts (Fig. 3d), and comparable to island-arc basalt. There is a corresponding relative enrichment in Ba, as indicated by high Ba/Nb and Ba/La ratios. The arc basalts and basaltic andesites have comparatively small Eu anomalies, which may be either positive or negative (Fig. 3a), and low *HREE* contents (most <10 × chondrites).

Values of Nb/Ta are ~13–17 for the arc basalts and basaltic andesites in the present study (Fig. 4a). As in HAOT, many of these ratios are sub-chondritic. Low Nb/Ta ratios are not unique to the Cascade arc, as Plank & White (1995) reported Nb/Ta ratios down to 6 in ICP–MS characterization of arc basalts. The low ratios may reflect prior extraction of melt from the source (Plank & White 1995) and preferential retention of Nb relative to Ta in rutile during dehydration of a subducting slab, resulting in lowering of Nb/Ta in the overlying mantle wedge (Green 1995). The latter suggestion is based on rutile – aqueous fluid partition coefficients, where D^{Nb}/D^{Ta} is nominally >1 in results of many, but not all, experiments reported by Brenan *et al.* (1994); note, however, that D^{Nb}/D^{Ta} is generally indistinguishable from 1 if published analytical uncertainty is considered.

The arc lavas are relatively oxidized, as found elsewhere by others (*e.g.*, Gill 1981). Values of FeO/FeO* range from 0.9 for the most primitive samples of HAOT to 0.6 for some of the arc rocks (Fig. 4b). Presumably, the arc signature is correlated with an increase in pre-eruption H_2O content (*e.g.*, Sisson & Layne 1993, Stolper & Newman 1994). The more oxidized nature of the arc rocks probably reflects relative pre-eruptive oxidation state and is unlikely to be related to degassing of the more hydrous magmas (Carmichael 1991). Water transported to the mantle wedge by subduction probably is responsible for oxidation of the source region of arc magmas (Brandon & Draper 1996).

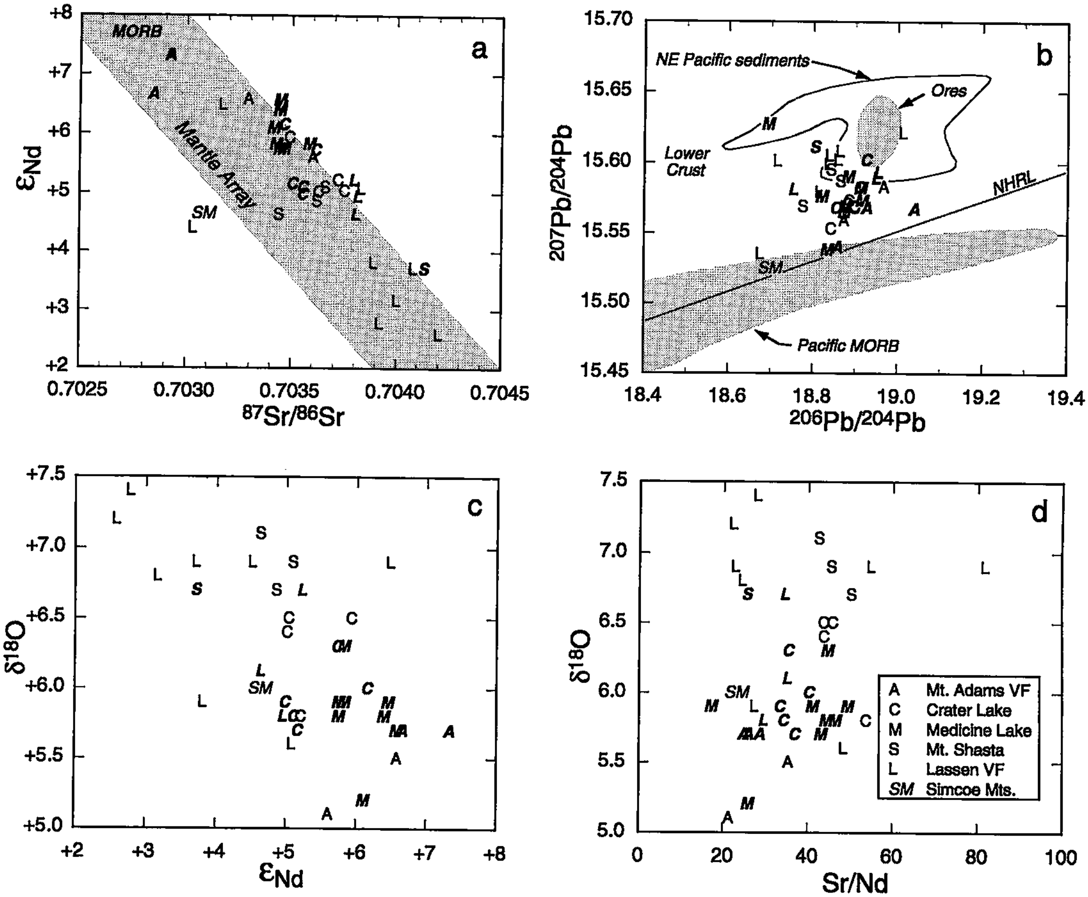

FIG. 5. Selected isotopic parameters. a) $^{87}Sr/^{86}Sr$ *versus* ε_{Nd}. Most samples plot in a small region approximately within the conservatively drawn mantle array (from Leeman *et al.* 1990, Fig. 10), Mount Adams samples high, Lassen and Shasta low. The Lassen sample with $^{87}Sr/^{86}Sr = 0.70305$ (below the mantle array) is magnesian basaltic andesite (sample LC86–1009; 58% SiO_2). b) Pb isotope correlation diagram. As in most arcs, data can be interpreted as mixtures of MORB-like Pb and Pb from marine sediments or, possibly, continental crust. Medicine Lake sample with highest $^{207}Pb/^{204}Pb$ is most primitive HAOT, which suggests that this Pb is mainly derived from subducted sediment. Note that the Simcoe Mountains sample, which represents a melt of intraplate-type mantle, plots on the *NHRL* [northern hemisphere regression line for oceanic basalts from Hart (1984)], and thus has an OIB affinity (nearby Lassen sample is LC86–1009). Field of *NE Pacific sediments* from Church (1976), Cascade *Ores* from Church *et al.* (1986), and *Pacific MORB* from White *et al.* (1987). *Lower Crust* represents maximum likely values ["0–250 Ma tectonothermal age lower crust" of Rudnick & Goldstein (1990)]. c) ε_{Nd} *versus* whole-rock $\delta^{18}O$. Shasta and, commonly, Lassen samples have high $\delta^{18}O$ and low ε_{Nd} values. Crater Lake samples with $\delta^{18}O > +6.0‰$ are basaltic andesites and an evolved HAOT. d) Sr/Nd *versus* $\delta^{18}O$. Arc magmas have higher Sr/Nd ratios than oceanic basalts and "average" continental crust. If high-$\delta^{18}O$ values for Shasta and Lassen samples were related to a subduction-derived component, these rocks should have high Sr/Nd ratios, which many do not.

Intraplate basalt

Basalt with a strong intraplate chemical signature of *LILE* enrichment in the absence of Nb–Ta depletion is limited in our data set to the sample from the Simcoe Mountains volcanic field (*SM* in figures). However, primitive lavas from the Lassen and Mount Adams volcanic fields contain hints of an intraplate component (Fig. 3b; Bullen & Clynne 1989, Leeman *et al.* 1990). The Simcoe Mountains sample is from an ejecta ring that contains mantle xenoliths. Although few lavas are as strongly alkaline as the Simcoe units, Quaternary alkali basalt vents are not restricted to the back arc, but occur in a 150 km east–west belt across the Cascade arc in southern Washington.

Mantle Components Implied by End-Member Magmas

Compositions of primitive Cascade lavas suggest blending of melts from, or mixing of, end-member geochemical domains in their mantle sources. Consideration of data for moderately evolved lavas (≥6% MgO) along with the set of primitive rocks analyzed here strengthens the case for a minimum of three end-member primitive liquids that reflect components of the mantle beneath the Cascades: depleted sub-arc mantle, a subduction component, and intraplate mantle.

Trace-element ratios

Following Leeman *et al.* (1990), we have plotted Nb/Zr *versus* Ba/Zr (Fig. 4c) to illustrate some of the effects of mixing of three end-member magma types or mantle components. A large number of high-quality analyses for Nb in specimens from the Crater Lake area suggest that there is no intraplate mantle present there, as all data trend directly from primitive HAOT toward IAB and pelagic sediment at nearly constant Nb/Zr. Note that all samples from the Mount Adams and a few from the Lassen volcanic fields are displaced to slightly higher Nb/Zr values, relative to the Crater Lake trend, and the Simcoe Mountains sample lies at higher Nb/Zr than Kilauea basalt.

The number of data points available for plotting increases considerably when INAA results are used in a plot of Ta/Yb *versus* Th/Yb (Fig. 4d). The large numbers of data points for Medicine Lake, Crater Lake, Lassen, and Mount Adams volcanic suites define fields that show the same trends as in Figure 4c. The INAA data confirm the lack of an intraplate (high Ta/Yb) signature at Crater Lake, suggest that one is weakly present at Medicine Lake, and add a few samples to the Lassen and Mount Adams fields that reflect mixing of all three end-members. Alternatively, crustal contamination could result in values intermediate between arc and intraplate trends, because the Ta/Yb ratio of average crust is higher than in arc lavas (Taylor & McLennan 1995). However, the slopes of the lower field boundaries for the three centers are remarkably consistent in Figure 4d and cannot be explained by addition of crustal material.

Isotopic composition

The primitive lavas of the present study plot within or very close to the conservatively drawn mantle array (after Leeman *et al.* 1990) on the $^{87}Sr/^{86}Sr$ *versus* ε_{Nd} diagram (Fig. 5a). Regional differences in isotopic composition (discussed below) and the limited number of primitive samples analyzed from each center preclude definitive statements about isotopic compositions of end-member mantle components. The lowest $^{87}Sr/^{86}Sr$ and highest $^{143}Nd/^{144}Nd$ ratios were measured for samples of HAOT from the Mount Adams field, but most have values comparable to those for arc basalt and basaltic andesite. Lavas with particularly high $^{87}Sr/^{86}Sr$ and low $^{143}Nd/^{144}Nd$ ratios may be contaminated. Borg *et al.* (1997) suggested that lavas from the Lassen area that plot below the mantle array (*e.g.*, magnesian basaltic andesite LC86–1009, Fig. 5a) contain a large fraction of fluid-transported Sr, but not Nd, derived from metabasalt of the subducted slab; this sample also has MORB-like Pb isotopic ratios. Note, however, that the alkali basalt from the Simcoe Mountains has a similar isotopic composition of Sr, Nd, and Pb (Figs. 5a, b), as though such features also may be intrinsic to intraplate mantle.

The isotopic composition of Pb is sensitive to crustal contamination, particularly in HAOT, where the base-level concentration is <1 ppm. Nearly all samples have higher $^{207}Pb/^{204}Pb$ ratios than the northern hemisphere regression line and Pacific MORB on a $^{206}Pb/^{204}Pb$ *versus* $^{207}Pb/^{204}Pb$ diagram (Fig. 5b). The Pb-isotopic trend toward fields for northeast Pacific sediments and Cascade ores may reflect crustal contamination or Pb derived from (not necessarily recently) subducted sediment. A modern sedimentary component should produce a positive correlation between the Pb isotope ratios. Miller *et al.* (1994) reported a strong negative correlation between $^{207}Pb/^{204}Pb$ and Ce/Pb ratios for Umnak in the Aleutians, and interpreted this as evidence for fluid-transported mantle Pb. Our Cascade data have the low Ce/Pb ratios typical of arcs, but possess only a weak negative correlation overall between $^{207}Pb/^{204}Pb$ and Ce/Pb ratios.

Oxygen isotope ratios show a good correlation with geological setting, as $\delta^{18}O$ values ≥ +6.5‰ are limited to the Lassen and Shasta areas, where Klamath – Sierra Nevada basement is known to be present. That values between +5.6 and +6.1‰ also occur at Lassen, along with the negative correlation between $\delta^{18}O$ and ε_{Nd} (Fig. 5c) in the data set as a whole, suggests that the high $\delta^{18}O$ and low ε_{Nd} values may be due to assimilation of crust. Implications of regional isotopic variation are discussed further below.

Chemical Characteristics of the Five Centers: Element-Abundance Diagrams

Element-abundance diagrams (Fig. 6) highlight chemical similarities and differences among the centers. These plots also provide for comparison with examples of primitive lava compositions from ocean ridge, island arc, and intraplate settings (Fig. 6f, N–MORB, E–MORB, IAB, OIB) that aid in identification of geochemical signatures of mantle components. Also evident are effects

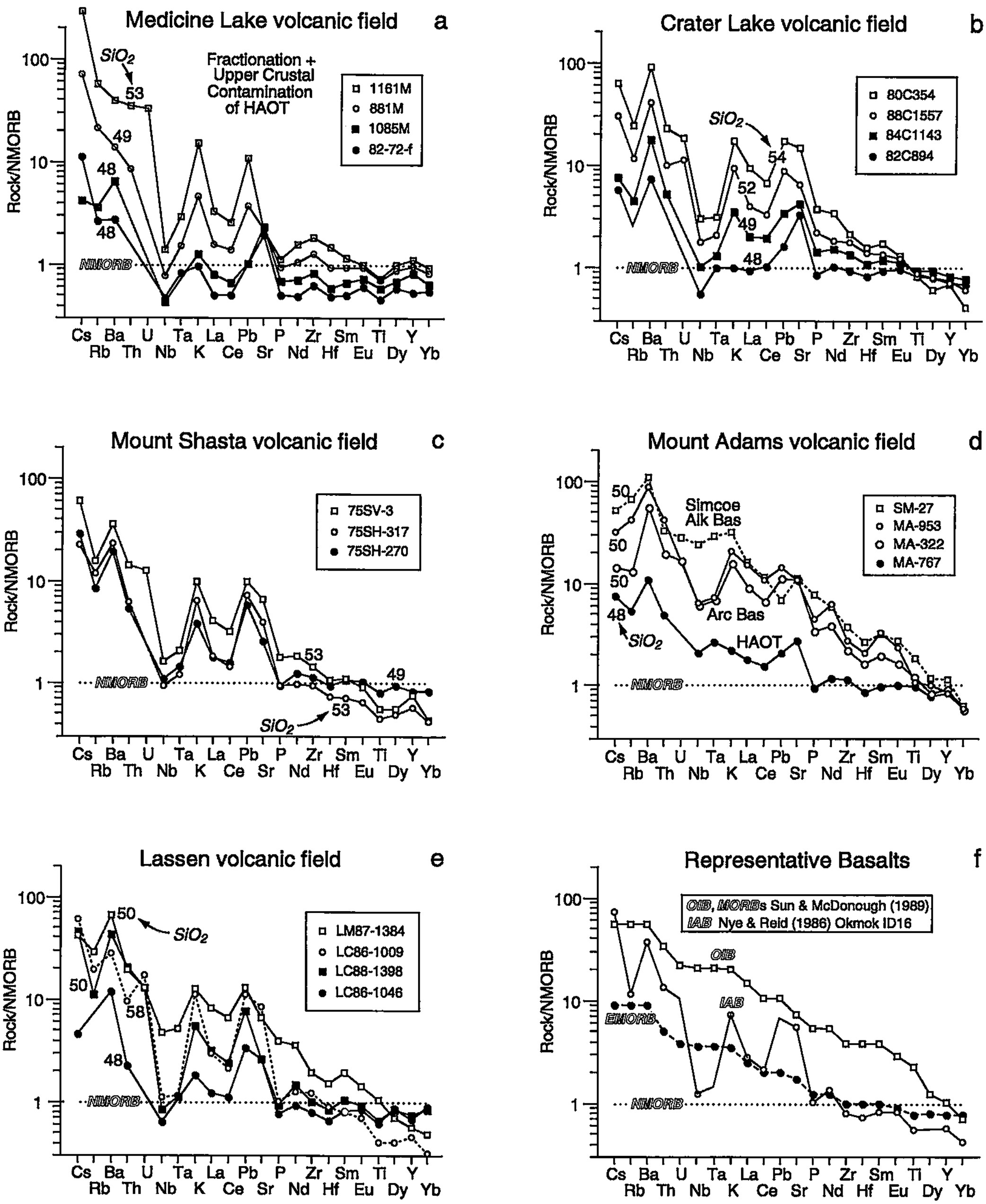

FIG. 6. Element-abundance diagrams for the five volcanic fields of this study and representative N-MORB, E-MORB, IAB, and OIB (sources of data as in other figures). Normalization values from Sun & McDonough (1989). Filled symbols are HAOT, and open symbols represent arc basalt and basaltic andesite, and alkali basalt. SiO_2 contents indicated for Cascade lavas (recalculated to sum to 100 wt.% volatile-free and with all Fe as FeO*). The effects of fractionation of HAOT and contamination with granite in the upper crust are shown by four samples from the Giant Crater lava field at Medicine Lake (differentiated and contaminated HAOT plotted with open symbols). Base-level HAOT has N-MORB-like abundances of most incompatible elements, but is enriched in *LILE*, as are samples of HAOT at the other centers. Crater Lake, Shasta, and Lassen samples form a continuum of compositions from HAOT to arc basaltic andesite. Magnesian basaltic andesite from Lassen (LC86–1009; dashed pattern), an extreme example of the arc signature, is strongly depleted in elements at the right of the diagram. Alkali basalt from the Simcoe Mountains has an OIB-like (intraplate) pattern. Arc basalt from Mount Adams and a basalt from Lassen also have steep patterns and comparatively small Nb–Ta "wells" suggestive of an intraplate component.

of processes such as assimilation of rocks derived from the upper crust.

Medicine Lake volcano

Four representative samples from the Giant Crater lava field of the Medicine Lake volcano (Fig. 6a) illustrate the effects of fractionation and crustal assimilation on the trace-element pattern of primitive HAOT (Donnelly-Nolan *et al.* 1991, Baker *et al.* 1991). The least differentiated rock (82–72–f; studied by Bartels *et al.* 1991) has *HFSE* and *HREE* abundances ~0.5× the Sun & McDonough (1989) N–MORB values, and is the most incompatible-element-depleted sample in our data set. Even this primitive rock, however, has elevated concentrations of some *LILE* relative to the other incompatible elements. The other three samples display a systematic increase in incompatible elements, except for Sr. Baker *et al.* (1991) described how the variation in composition of the Giant Crater lavas is due to fractionation of HAOT plus assimilation of granite in the upper crust. This scenario is consistent with the patterns in Figure 6a, where increases in Sr, Eu, and Ti are suppressed. Note also that the *HREE* and most elements on the right side of the diagram increase in an approximately parallel fashion, and that Ba is not enriched relative to Th and Rb in the two most-evolved samples (*cf.* IAB in Figure 6f).

Crater Lake

The four samples from the Crater Lake area illustrate the effect of blending HAOT and arc magmas or their source components (Bacon 1990, Bacon *et al.* 1994) in the absence of an intraplate component or contamination with felsic material (Fig. 6b). The most primitive HAOT has *HFSE* and *REE* abundances comparable to N–MORB, except that Nb is lower in the Crater Lake rock. Other than K, the concentrations of the *LILE* are elevated, as at Medicine Lake. The other samples, which range from differentiated HAOT to magnesian basaltic andesite, display a systematic enrichment in all elements to the left of Ti and a concomitant decrease in *HREE* and Y; *i.e.*, as the lavas become richer in incompatible elements, the arc signature becomes more pronounced, and concentrations of the moderately incompatible elements decrease. This observation applies in a general way to Crater Lake, Shasta, and Lassen.

Mount Shasta area

The three samples from the Mount Shasta area plotted in Figure 6c can be interpreted in the same way as those from Crater Lake. The HAOT is more differentiated than the most primitive rocks from Medicine Lake or Crater Lake, but still has the relatively flat P–Yb pattern. The two samples of basaltic andesite show enhancement of the arc signature, including relative depletion in *HREE* and Y. Note the high Pb/Sr ratios of the Shasta area lavas. Samples of HAOT and magnesian basaltic andesite from the Shasta region described by Baker *et al.* (1994) have similar N–MORB-normalized patterns to those in Figure 6c.

Mount Adams volcanic field

All three components are present in the Mount Adams volcanic field samples (Fig. 6d), as also found by Leeman *et al.* (1990) for the southern Washington Cascades taken as a whole. The Simcoe Mountains sample has a clear intraplate signature, as stated previously. The high Nb and Ta concentrations in the sample of HAOT plotted may result from presence of intraplate-type mantle in its source. Arc basalt shows a moderate Nb–Ta "well", overall low concentrations of the *HFSE*, comparatively high Pb/Sr ratio, and *HREE* depletion typical of other samples rich in a subduction component.

Lassen volcanic field

The Lassen volcanic center and surrounding region contain many vents and a great variety of mafic lavas (Bullen & Clynne 1989, Clynne 1993, Borg *et al.* 1997). The three components are present at Lassen as in southern Washington. Primitive HAOT is much like that at Crater Lake but for its higher Pb/Sr ratio and slight K enrichment. True alkali basalt does not occur at Lassen, but intraplate mantle is clearly represented (Fig. 4d), and may be responsible for the relatively shallow Nb–Ta "well" and high Ti of sample LM87–1384 (Fig. 6e). There is no question of a strong arc signature in many of the Lassen volcanic field lavas. It is most striking in magnesian basaltic andesite (dotted line), which has a pattern very much like that of primitive IAB (Fig. 6f), yet contains 58% SiO_2 at an Mg# of 71.

Chemical Characteristics of the Five Centers: *REE* Patterns

Isotope-dilution analyses for the *REE* are sufficiently precise that subtleties of chondrite-normalized patterns are meaningful and can be interpreted in terms of processes and mantle sources. Patterns are presented in Figure 7 for the same samples as are plotted in Figure 6.

Medicine Lake volcano

The convex-upward pattern of the most primitive HAOT from Giant Crater (Fig. 7a) is similar to that of N–MORB (Fig. 7f), although *REE* concentrations are lower overall in the Medicine Lake rock. The positive Eu anomaly is pronounced. With fractionation of basaltic magma and assimilation of granite, the *REE* abundances increase, the *LREE* become fractionated, the

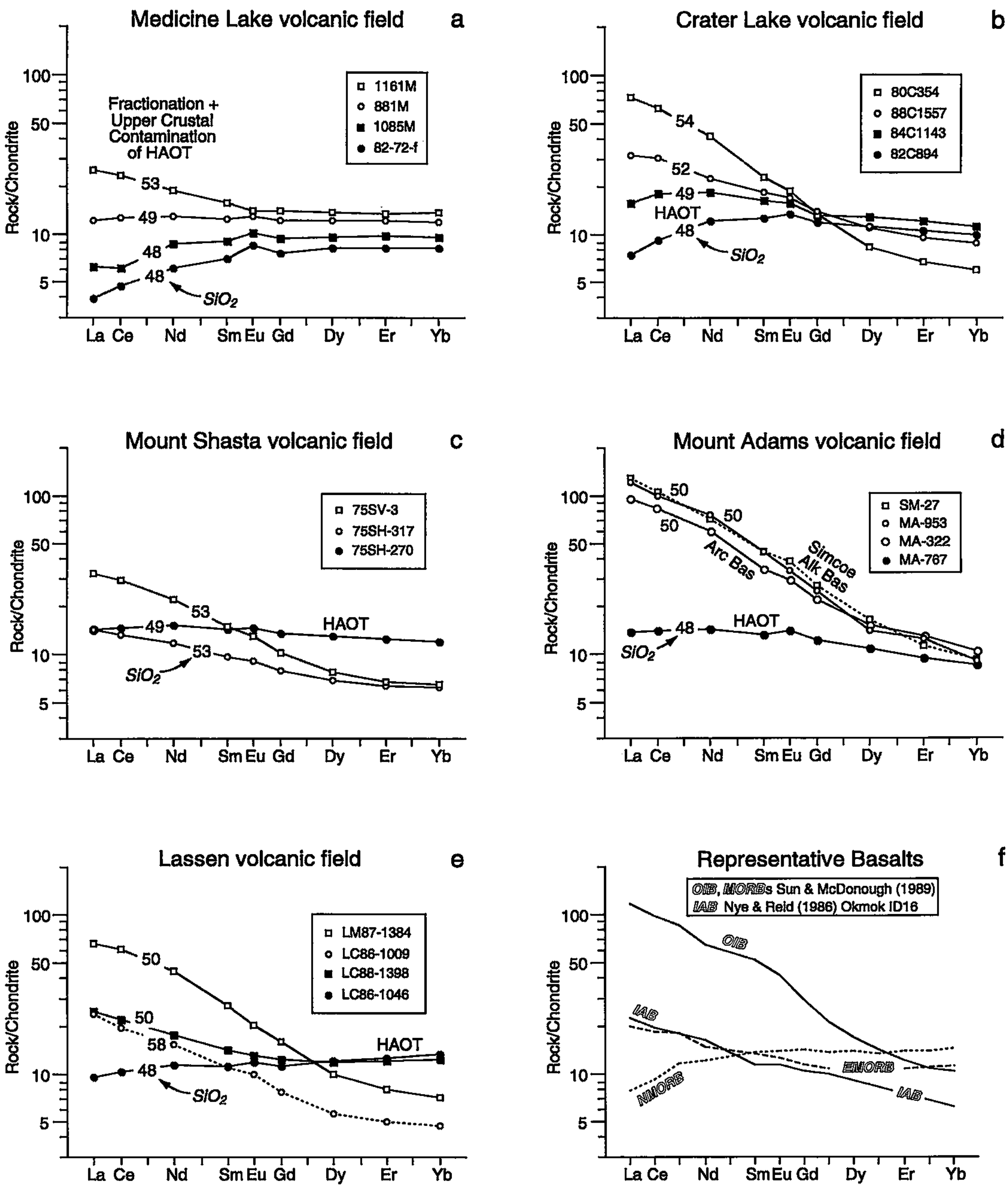

FIG. 7. Isotope-dilution *REE* data for samples plotted in Figure 6 normalized to the C–1 chondrite values of Sun & McDonough (1989). Symbols and SiO_2 contents as in Figure 6. Four samples from the Giant Crater Lava field, Medicine Lake, have decreasing Eu/Eu*, increasing *LREE* fractionation, and uniform increases in *HREE* with differentiation and contamination with granite. Negative Ce anomalies, as in 1085M, are present in other Medicine Lake lavas. *REE* patterns of Crater Lake samples change systematically from *LREE*-depleted HAOT with positive Eu anomaly to sigmoidal patterns in basaltic andesites. Similar patterns are found at Lassen and Shasta. Low abundances of the *HREE* in the arc basalt and basaltic andesite patterns suggest generally higher degrees of melting than for samples of HAOT. The sigmoidal shape of the *REE* pattern, which suggests an eclogitic residue, apparently is inherited from a subduction-derived component, possibly transported to the mantle wedge by a partial melt of the slab. Although the HAOT pattern at Mount Adams is like those elsewhere, arc basalt is similar to alkali basalt from the Simcoe Mountains.

HREE show a parallel rise, and the Eu anomaly decreases, becoming negative in the most evolved sample. Fractionation and contamination of the Giant Crater lavas thus result in *HREE* behavior unlike that in arc basalts and basaltic andesites of the other volcanic fields. In fact, lavas at the Medicine Lake volcano (and Mount Adams volcanic field) have relatively high abundances of the *HREE* overall: of 168 INAA determinations of *REE* concentrations in Medicine Lake samples with ≥6% MgO, only two have Yb_N less than 10 (J.M. Donnelly-Nolan, unpubl. data, 1995). This expanded data-set contains a few examples of "sigmoidal" *REE* patterns (see below), but with lower *LREE* and higher *HREE* than at Crater Lake. Patterns with monotonic slopes, as are common in lavas from Mount Adams, are rare and have comparatively gentle slopes ($30 < La_N < 50$).

The precision of the isotope-dilution analyses for the *REE* and replication by INAA indicate that the negative Ce anomaly in sample 1085M (and 1376M, Table 1) is real. The INAA data-set for Medicine Lake contains many samples with a negative Ce anomaly. The only other samples in this study with a negative Ce anomaly are two specimens of HAOT from Lassen. The presence of a negative Ce anomaly in island-arc lavas has been attributed to subduction of pelagic sediment (White & Patchett 1984, Hole *et al.* 1984). It may be that the negative Ce anomaly results from comparatively ancient (Mesozoic?) sediment subduction that locally affected the HAOT source, and that is not evident in arc basalt and basaltic andesite because of an overwhelming contribution from modern subduction, in which pelagic sediment is not well represented.

Crater Lake

The *REE* patterns for the four samples in Figure 7b from the Crater Lake area rotate about a point near Tb, as noted previously for HAOT and calc-alkaline basaltic andesites (Bacon 1990). Primitive HAOT has an N–MORB-like pattern and also the strongly positive Eu anomaly typical of end-member HAOT. Differentiated HAOT (84C1143) has higher *REE* abundances overall and, although still convex upward, is slightly *LREE*-enriched. Arc basalt and magnesian basaltic andesite show a progressive increase in *LREE* and decrease in *HREE* while retaining a small positive Eu anomaly. These samples have a sigmoidal pattern: convex-upward *LREE* and concave-upward *HREE*. The larger Crater Lake data-set of 76 samples with MgO ≥ 6% analyzed by INAA (Bruggman *et al.* 1989, C.R. Bacon, unpubl. data 1995) contains 18 examples having $Yb_N < 10$ and several with a sigmoidal pattern.

Mount Shasta area

The one sample of HAOT from the Mount Shasta area has a flat *REE* pattern with small positive Eu anomaly at a little more than 10× chondrites (Fig. 7c). The basaltic andesites have lower levels of the *HREE* than the HAOT, a small positive Eu anomaly, and slight to moderate *LREE* enrichment. Sample 75SV–3 has a sigmoidal pattern like magnesian basaltic andesite from Crater Lake, but with less pronounced *LREE* enrichment.

Mount Adams volcanic field

The *REE* pattern for HAOT from the Mount Adams volcanic field (Fig. 7d) is similar to that of HAOT from the other centers. Alkali basalt from the Simcoe Mountains volcanic field has a steep, straight pattern. Surprisingly, arc basalt has a nearly identical pattern, including Yb at ~10× chondrite, and lacking upward concavity in the *HREE* pattern as found in lavas with arc signature at the other centers. A search of 48 INAA results of rocks with MgO ≥ 6% (W. Hildreth & J. Fierstein, unpubl. data, 1995) found three with sigmoidal patterns, and only one with $Yb_N < 10$.

Lassen volcanic field

As expected on the basis of element-abundance patterns, the four representative samples from the Lassen volcanic field in Figure 7e show a wide range of *REE* patterns. HAOT is similar to its relatives at the other centers. Sample LC88–1398 is arc basalt on the basis of chemical composition, but it has HAOT-like compositions of the phenocrysts (Clynne 1993). It has similar *HREE*, but notably higher *LREE* concentrations, than primitive HAOT. This sample also has high *LILE* (except Sr) concentrations, high $^{87}Sr/^{86}Sr$, $^{207}Pb/^{204}Pb$, $\delta^{18}O$, and low $^{143}Nd/^{144}Nd$ values. Arc basalt has a sigmoidal pattern similar to magnesian basaltic andesite from Crater Lake. The magnesian basaltic andesite from the Lassen field, although characterized by a similarly shaped pattern, has much lower abundances of the *REE*, in keeping with its incompatible-element-poor overall composition. Positive Eu anomalies are small or lacking in the Lassen area samples. In the examples in Figure 7e, and in a larger data-set of 42 compositions of rocks with MgO ≥ 6% (Clynne 1993), there is no sample with the straight, fractionated pattern shown by alkali basalt from the Simcoe Mountains, as might be anticipated to be found on the basis of the other trace-element evidence for an intraplate component (Fig. 4d). As at Crater Lake, some samples from the Lassen area have relatively low *HREE* contents (10 of 42 have $Yb_N < 10$).

Regional Differences in the Composition of Primitive Lavas

Description of the compositions of primitive lavas from the five centers has touched upon systematic regional variations in abundances of the incompatible

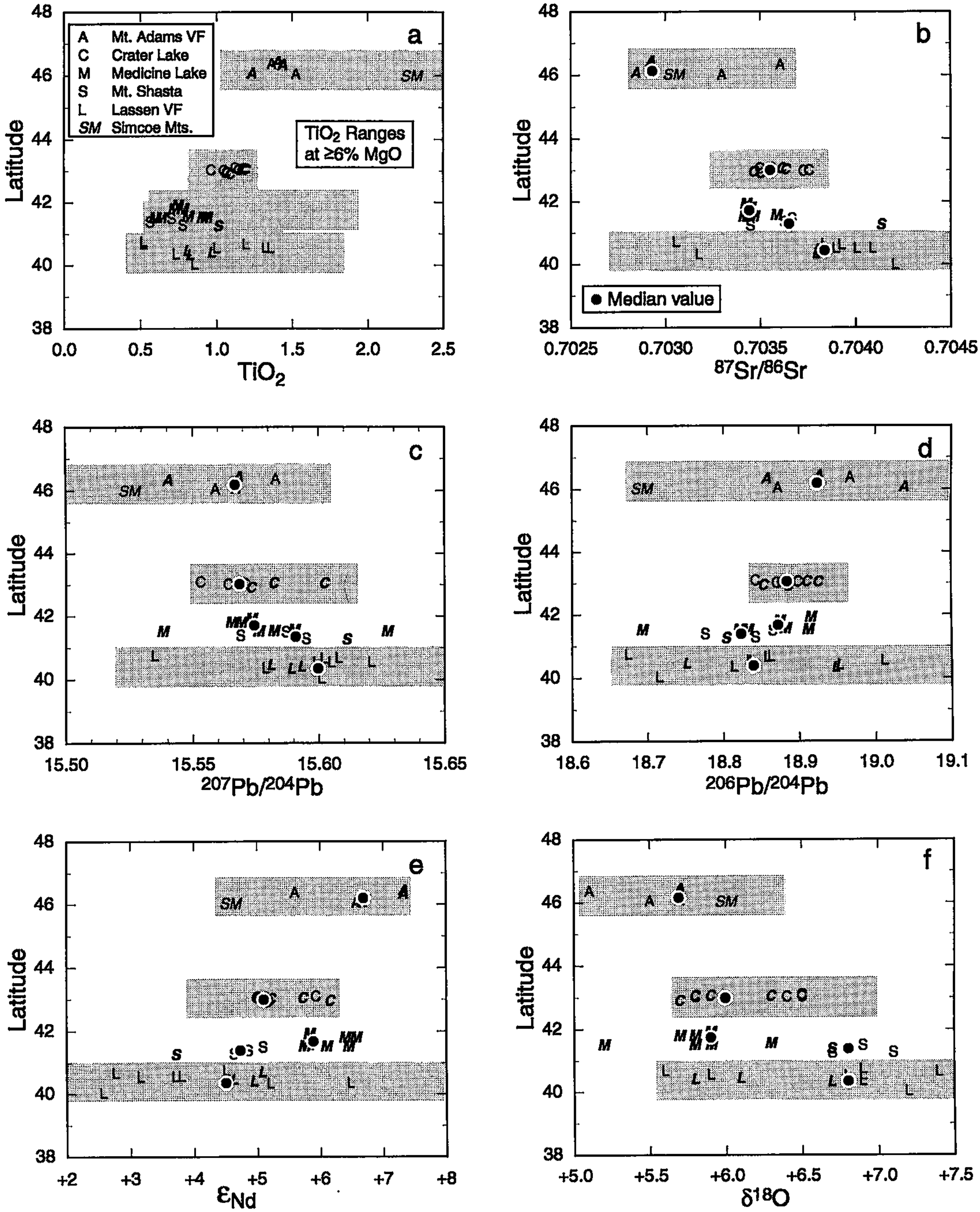

FIG. 8. TiO_2 contents and selected isotope ratios *versus* latitude. Shaded fields indicate ranges of literature data [isotopic data for Mount Adams from Leeman *et al.* (1990), Crater Lake from Bacon *et al.* (1994), Lassen from Bullen & Clynne (1990) and unpublished data, 1995; TiO_2 contents from Baker *et al.* (1994) and sources listed for Fig. 4d]. Note increase in minimum TiO_2 content from south to north, and regional differences in median values (dots) of isotope ratios for data of this study (letters).

elements and isotopic compositions. Here, we plot and discuss selected geochemical parameters as functions of latitude in order to focus on the more significant features of regional variation.

Variations in TiO_2 content and various isotopic ratios are plotted *versus* latitude in Figure 8. Also shown are fields defined by our own unpublished data and literature values for the Mount Adams, Crater Lake, and Lassen areas. Available isotopic data for Shasta and Medicine Lake are insufficient for meaningful definition of ranges of values. Of the others, Crater Lake has the narrowest range of isotopic compositions.

HFSE and Fe

There are the most data for Ti among the *HFSE*. Minimum TiO_2 contents at MgO ≥ 6% increase by a factor of two from south to north (Fig. 8a). Crater Lake has the most restricted range of concentrations, in keeping with the lack of an observed *HFSE*-rich intraplate contribution. Maximum TiO_2 values at Medicine Lake (1.9%), Lassen (1.8%), and Mount Adams (2.5%) are similar to those of intraplate basalts. Mount Adams also has higher concentrations of other *HFSE* and Fe than the centers to the south. The relatively high *HFSE* contents of basalts from the Mount St. Helens, Indian Heaven, and Mount Adams volcanic fields were noted by Leeman *et al.* (1990).

REE

All five centers have HAOT with *LREE*-depleted to slightly *LREE*-enriched chondrite-normalized patterns, with a positive Eu anomaly. A negative Ce anomaly is present in some samples of HAOT, and is particularly common at Medicine Lake. "Sigmoidal" *LREE*-enriched patterns with convex-upward *LREE*, concave-upward *HREE*, and $Yb_N < 10$ are common at Crater Lake, Shasta, and Lassen. Patterns with monotonic steep negative slopes and $Yb_N \sim 10$ are common only at Mount Adams.

Sr, Pb, Nd, and O isotopes

The range in Sr isotopic composition is well defined by the expanded data-sets for the Mount Adams, Crater Lake, and Lassen volcanic fields, which include results published elsewhere. Of these, Lassen shows the greatest variation. Note that the fields for $^{87}Sr/^{86}Sr$ in Figure 8b contain a few samples of andesite with <6% MgO and low $^{87}Sr/^{86}Sr$ ratios; these samples are believed to have had a low-$^{87}Sr/^{86}Sr$ basaltic parent not represented among erupted lavas (*e.g.*, Bacon *et al.* 1994). The primitive lavas analyzed in the present study have *median* $^{87}Sr/^{86}Sr$ ratios that tend to decrease from south to north.

Lead isotopic compositions show broad overlap among the Cascade centers. However, values for the primitive lavas of this study again suggest regional differences. In this case, $^{207}Pb/^{204}Pb$ tends to be higher and $^{206}Pb/^{204}Pb$ lower in the south (Figs. 8c, d). This crude anti-correlation between Pb isotope ratios may reflect crustal contamination of lavas erupted in California, or it may be an artifact of inadequate coverage in the present data-set. Lower crust would be expected to have low $^{238}U/^{204}Pb$, and hence comparatively low $^{206}Pb/^{204}Pb$ (as seen at Lassen) if sufficiently old.

Minimum ε_{Nd} values show a general increase from south to north (Fig. 8e), with Medicine Lake being restricted to relatively high values, perhaps because of the limited coverage in this data set. The trend is defined by relatively low ε_{Nd} of the Lassen and Shasta samples.

A clear regional trend is shown by maximum $\delta^{18}O$ values (Fig. 8f). The highest $\delta^{18}O$ values in primitive rocks occur in the south, and median values generally decrease to the north. All centers except Shasta, where data are limited to four samples, have some values in the normal mantle range of +5.5 ± 0.4‰ (Mattey *et al.* 1994) and at or below the base-level of +5.9 to +6.2‰ for arc basalts suggested by Harmon & Hoefs (1995). Mattey *et al.* (1994) suggested that at the lowest solidus temperatures considered likely for peridotite, allowing for the largest mineral–melt fractionations, the maximum $\delta^{18}O$ values of basaltic liquids in equilibrium with peridotitic mantle would be in the range +6.0 – +6.5‰. Causes of ^{18}O enrichment are suggested below.

Regional Differences in Basement Rocks and Crustal Contamination

Regional differences in geochemical parameters that are sensitive to contamination suggest that many primitive lavas record some degree of crustal interaction (*e.g.*, Bacon *et al.* 1994). The most compelling evidence for this interaction in the data gathered for this study is the commonly high $\delta^{18}O$ values of samples from the Shasta and Lassen areas. The high $\delta^{18}O$ values might result from surface processes, although this seems unlikely given the restriction of $\delta^{18}O$ values ≥ +6.5‰ to the Lassen and Shasta volcanic fields and the large proportion of ^{18}O-rich samples there (11 of 15). Chemically primitive lavas with $^{87}Sr/^{86}Sr$ ratios ≥ 0.704, only present at Lassen and Shasta, also have $\delta^{18}O$ ≥ +6.7‰. These samples commonly have high $^{207}Pb/^{204}Pb$ values, coupled with low $^{206}Pb/^{204}Pb$ and ε_{Nd} values (*e.g.*, LC88–1398), which are consistent with contamination with lower crust characterized by ancient depletion in U. Potential assimilants or reactive wallrocks would have to be altered mafic or ultramafic rocks with comparatively high $\delta^{18}O$ values (+8 – +12‰), as may be present in the Klamath Mountains basement [see summary in Bacon *et al.* (1994, p. 1550)], in order to produce the required shift in $\delta^{18}O$ without notably decreasing Mg# or concentrations of compatible trace-elements in the resulting magmas.

Regional geophysical surveys suggest a cause for the elevated $\delta^{18}O$ values for the Shasta and Lassen area volcanic rocks. Isostatic residual gravity highs immediately west of the Shasta and Lassen volcanic fields (Blakely *et al.* 1985, Blakely & Jachens 1990) approximately coincide with high P-wave velocities in the crust (Benz *et al.* 1992) and imply that thick sequences of mafic or ultramafic (ophiolitic) rocks (or both) project beneath Mount Shasta and probably also Lassen. North of Mount Shasta, where increases in $\delta^{18}O$ of primitive lavas relative to presumed mantle values are smaller (Fig. 8; Bacon *et al.* 1994), the continuation of the belt of gravity highs is west of the Cascades and merges with the Oregon Coast Ranges (Blakely & Jachens 1990), where the rocks responsible for it would have no effect on the modern arc. Results of seismic refraction surveys (Fuis *et al.* 1987, Fig. 11) indicate that the Ordovician Trinity ultramafic sheet is present in the upper crust as deep as ~10 km beneath Mount Shasta and that a 7.0 km/s layer, possibly consisting of ophiolitic rocks, begins ~17 km beneath the surface. To the east, beneath Medicine Lake, where high-^{18}O primitive lavas have not been reported, Fuis *et al.* (1987) did not identify the Trinity ultramafic sheet and found that a 7.0 km/s layer is not reached until a depth of ~27 km.

It has been suggested that the subduction component is the carrier of excess ^{18}O in some arc lavas (*e.g.*, Ito & Stern 1985/86, Woodhead *et al.* 1987). Borg *et al.* (1997) propose that the high $\delta^{18}O$ values for lavas from the Lassen area reflect their mantle source, which was modified by a high-^{18}O subduction component. Laser-fluorination O-isotopic analyses of mantle minerals strongly suggest that the mantle is quite uniform in its O-isotopic composition, regardless of the presence of hydrous phases, casting doubt on subduction-related increases in the $\delta^{18}O$ value of the mantle wedge (Mattey *et al.* 1994). The Sr/Nd ratio, which is likely to be lower in continental and oceanic crustal rocks than in arc magmas (Rudnick 1995), can be used to test the hypothesis that the subduction component is responsible for high-$\delta^{18}O$ lavas of the Shasta and Lassen areas. Were the subduction component responsible for elevated $\delta^{18}O$ values, samples with high $\delta^{18}O$ would have high Sr/Nd ratios. Because there is no correlation between $\delta^{18}O$ and Sr/Nd [or Sr/P, used as an index by Borg *et al.* (1997)], and because many of the high-^{18}O lavas also have Sr/Nd ratios of only ~20–30 (Fig. 5d), far lower than samples with a strong subduction-related geochemical signature (Sr/Nd as high as 82), a contamination process is the more likely explanation for the high $\delta^{18}O$ values. Any plagioclase fractionation that might accompany contamination would further reduce Sr/Nd for a given increase in $\delta^{18}O$.

Our data for Medicine Lake include four samples from the Giant Crater lava field, where assimilation is known to be important, but the contaminant is granite of the upper crust (Grove *et al.* 1988, Baker *et al.* 1991) that probably is Cenozoic in age. The most contaminated and differentiated of these Giant Crater samples (1161M) has a $\delta^{18}O$ value of +5.9‰, whereas one sample of basalt (881M) has an anomalously low $\delta^{18}O$ value of +5.2‰. Definitive O-isotopic evidence for a basement-contamination effect is lacking in southern Washington, even though Mount Adams is only ~40 km south of exposures of pre-Tertiary rocks. One sample from the Mount Adams area (MA–953) has a $\delta^{18}O$ value of only +5.1‰. Contamination with a small amount of low-^{18}O rock from the upper crust may explain the $\delta^{18}O$ values of these samples. Alternatively, the low-^{18}O samples may simply reflect variation within the mantle, because these values are within the range defined by mantle peridotites (Mattey *et al.* 1994).

Although we have presented isotopic data that are readily interpreted in terms of crustal contamination, geochemical evidence for contamination is not always separable from the effects of subduction in the Cascade province. This is a direct result of the fact that the basement rocks consist of accreted oceanic and arc terranes stitched together by tonalite–granodiorite plutons, all of which have suffered the effects of Late Cenozoic magmatism and associated hydrothermal activity that have added to and re-processed the crust. Thus, the age of a subduction component identified in the geochemistry of primitive lavas can be somewhat ambiguous, at least in the HAOT source, as discussed below.

Source Characteristics

Many authors have pointed out that HAOT and arc lavas cannot be related by any reasonable combination of fractionation, assimilation, or melting of a common source (*e.g.*, Hughes & Taylor 1986, Bacon 1990, Baker *et al.* 1994). The compositional spectrum results from variation in extent of melting of mantle sources that are variably enriched in a subduction component and have a range in capacity to produce basaltic melt (*i.e.*, fertility).

Temperature, depth, and water content

The origin of HAOT liquids is relatively straightforward. Bartels *et al.* (1991) conducted phase-equilibrium experiments on primitive HAOT from Medicine Lake, including sample 82–72–f. They found that nominally anhydrous HAOT is in equilibrium with a spinel lherzolite assemblage at ~1290°C at 11 kbar, presumably the point of separation of HAOT magma from the mantle [recall that Sisson & Layne (1993) reported ≤0.3% dissolved H_2O in melt inclusions in olivine phenocrysts]. These pressure conditions correspond to a depth near the base of the crust (Mooney &

Weaver 1989). Baker *et al.* (1994) concluded that HAOT at Shasta (their high-alumina basalt) represents 6–10% nearly anhydrous melting of depleted mantle that had previously been enriched with a modest amount of subduction component (*e.g.*, Donnelly-Nolan *et al.* 1991). We accept this model, and suggest that other HAOT compositions in the northern California to southern Washington Cascades can be explained by combinations of variation in the amount of a subduction component added to the source and differences in degree of melting [owing primarily to source fertility, as reflected by amount of clinopyroxene (Clynne 1993), but also to H_2O content]. Positive Eu anomalies probably result from the reduced nature of HAOT and the presence of residual clinopyroxene (Donnelly-Nolan *et al.* 1991) at the site of last equilibration in the mantle. Higher Sc contents in HAOT in comparison with arc basalts and basaltic andesites also may reflect a larger contribution from clinopyroxene in the HAOT source, relative to the less fertile source of the arc magmas, in which all clinopyroxene may be consumed and Sc in melts thereafter diluted by high degrees of melting. Alternatively, residual garnet, if present in the source of the arc magmas but not in that of HAOT, would result in lower Sc contents of the arc magmas.

The origin of arc basalt and basaltic andesite is commonly linked to the effects of H_2O on melting in a subduction-component-enriched mantle. Morris & Hart (1983), Hickey *et al.* (1986), Luhr (1992), Stolper & Newman (1994), Baker *et al.* (1994), and others have suggested that melt fraction during genesis of arc basalt and basaltic andesite is a function of the H_2O content (and relative fertility) of the mantle source. High pre-eruptive H_2O contents of mafic arc magmas have been reported by Anderson (1974), Sisson & Layne (1993), and Sobolev & Chaussidon (1996). For example, Sisson & Layne (1993) documented up to 3.3% dissolved H_2O in melt inclusions in olivine from basaltic andesite erupted near Mount Shasta. Baker *et al.* (1994) summarized evidence for the importance of H_2O on extent of melting at upper mantle pressures and presented a model for the origin of calc-alkaline basalt and magnesian basaltic andesite of the Mount Shasta area. They argued that these magmas contained between 3.5 and 6% H_2O, last equilibrated with harzburgite at ~1200°C at *ca.* 10 kbar, and represent melting extents of up to ~30%. The comparatively low *HREE*, Y, and Sc contents of the arc lavas would be a result of high degrees of melting of a depleted, relatively infertile source that had been enriched in H_2O, *LILE*, and *LREE* by addition of a subduction component.

Origin of sigmoidal REE patterns

The sigmoidal *REE* patterns of arc basalt and basaltic andesite from Lassen, Shasta, and Crater Lake appear to be consistent with subduction-component enrichment of magma sources. The Quaternary absarokite described by Conrey *et al.* (1997; sample RC93–50) from the northern Oregon fore-arc provides an extreme example of a sigmoidal *REE* pattern in a subduction-component-rich primitive lava (Ce ~300×, Yb ~7× chondrites).

Generation of sigmoidal *REE* patterns cannot be modeled by melting spinel or garnet lherzolite (*e.g.*, Martin 1987) with either *LREE*-depleted or monotonically decreasing (negative slope) chondrite-normalized *REE* abundances, such as are characteristic of many peridotite xenoliths and massifs (McDonough & Frey 1989). Neither can fractional crystallization of liquids with such *REE* patterns produce the sigmoidal pattern because bulk distribution-coefficients for the *HREE* must be significantly greater than 1 and must decrease with increasing *REE* atomic number (limiting any role of garnet). Rather, melting and crystallization models require that the sigmoidal *REE* pattern be a characteristic of the source peridotite (Stern *et al.* 1989).

McCulloch & Gamble (1991) argued that fluid extracted from the subducted slab would carry *LREE* but that *HREE* would be retained in the slab. Addition of such a fluid-transported subduction component to depleted mantle could produce the required *REE* pattern that would yield melts with a sigmoidal *REE* pattern. Infertile peridotite xenoliths with a sigmoidal *REE* pattern and *LREE* 4–10× chondritic values have been described by Ionov *et al.* (1995), who suggested that these rocks had experienced large degrees of partial melting and melt extraction, followed by metasomatism by (*LREE*-bearing) fluids. Calculated compositions of partial melt for such metasomatized peridotites have a sigmoidal *REE* pattern and abundances similar to those observed in the Cascade lavas.

Alternatively, a slab-derived melt might carry a sigmoidal *REE* signature to the depleted mantle wedge. Support for this mechanism can be found in rocks of the tonalite – trondhjemite – granodiorite (TTG) suite, which commonly have sigmoidal *REE* patterns and are believed to be formed by partial melting of eclogite or garnet granulite (metabasalt), leaving a garnet + clinopyroxene ± amphibole residue (Arth & Hanson 1972, Arth *et al.* 1978, Drummond & Defant 1990, Rapp & Watson 1995). Note that we are not suggesting that primitive Cascade lavas are slab melts, only that such melts may be responsible for the sigmoidal character of *REE* patterns. In either case, fluid or melt transport, melting of peridotite in the wedge is incapable of producing the sigmoidal *REE* pattern without prior enrichment of that source by a slab-derived fluid or melt.

We favor a model in which variation in concentrations of SiO_2 and incompatible elements in arc basalt and basaltic andesite are tied to the amount of subduction-component enrichment, which, along with source fertility, determines the extent of melting at a given temperature and depth. This model is consistent with the adjacent occurrence of both HAOT and lavas with strong trace-element signatures of arc magmas. Note that the most silica-rich basaltic andesite (LC86–1009) has a sigmoidal *REE* pattern (Fig. 7), similar to arc basalt (LM87–1384), but relatively low abundances of all *REE* (and Sc), consistent with its origin as a high-degree melt, presumably leaving a harzburgitic residue, as suggested by Baker *et al.* (1994) for magnesian basaltic andesite at Shasta.

The steep, straight *REE* patterns and high *HREE* concentrations of our alkali basalt sample from the Simcoe volcanic field imply a low degree of melting of enriched mantle. Although the arc basalt from the Mount Adams volcanic field has a similar *REE* pattern (Fig. 7), we suggest that it has lower abundances of moderately incompatible elements because it represents a higher melt-fraction, enriched in a subduction component.

The Cascade Upper Mantle

Composition

We have presented compositional data indicative of at least three end-member primitive magmas at the five Cascade volcanoes studied. These imply three mantle components in the sources of HAOT, arc basalt and basaltic andesite, and intraplate basalt: depleted sub-arc mantle, mantle enriched by a modern subduction component, and OIB-source-like intraplate mantle. The sizes of domains within the mantle are unknown, but the spatial association of vents for all three lava types indicates either limited areal extent or a layered structure. It does not appear to be possible to discriminate between mixing of sources in the mantle and blending of melts from different sources in order to produce the continuum of lava compositions.

Universal presence of HAOT with minor *LILE* enrichment relative to N–MORB requires widespread depleted sub-arc mantle. The arc signature present in the HAOT source may be an old one, as HAOT with similar *LILE* enrichment (commonly including Cs ± Pb) is found far to the east of the modern Cascade arc, in the Oregon Plateau and northern Basin and Range region (Hart *et al.* 1984; W.K. Hart unpubl. data, 1995). This depleted sub-arc mantle corresponds to Carlson's (1984) C1 incompatible-element-depleted mantle reservoir east of the Cascades.

We suggest that the subduction signature, clearly present in arc basalt and basaltic andesite of the Cascades, is linked to modern subduction because these lavas are restricted to the arc itself and have much higher *LILE* abundances than samples of HAOT, which are considered to represent similar or lower degrees of melting. The actual source of arc basalt and basaltic andesite may be less fertile than that of HAOT (Baker *et al.* 1994, Clynne & Borg 1997), though it must be more hydrous. Clearly, some geochemical tracers are derived from subducted sediment, such as Cs and Pb. However, the few published $^{10}Be/^{9}Be$ data for Cascade lavas do not indicate a measurable contribution from young pelagic sediment. Low $^{10}Be/^{9}Be$ ratios and B concentrations in four lavas from the southwest Washington Cascades (Morris & Tera 1989, Leeman *et al.* 1990) probably reflect slow subduction of the young, hot Juan de Fuca plate plus sediment derived from the continental margin (^{10}Be- and B-poor), and consequent loss of fluid-transported elements during dehydration of the slab trenchward of the volcanic front. The proportion of the subduction component obtained from altered basaltic rocks of the slab is equivocal, as we do not find the negative correlation between $^{207}Pb/^{204}Pb$ and Ce/Pb ratio used by Miller *et al.* (1994) to identify mantle Pb derived from a subducted slab.

An intraplate mantle component is present in lavas from the Mount Adams and Lassen volcanic fields and appears also to be present in some rocks from Medicine Lake (Fig. 4d). At Lassen (Borg *et al.* 1997) and, apparently, Medicine Lake, the intraplate signature tends to increase to the east, whereas the arc character decreases. Hughes (1990) found geochemical evidence for both depleted and OIB-source-like mantle beneath the central Oregon Cascades (approximate lat. 44°–45°N, north of Crater Lake), Conrey *et al.* (1997) reported within-plate basalts from northern Oregon and southern Washington, and some analyses of basaltic andesite from the Mount Bachelor chain (lat. 44°N) reported by Gardner (1994) also have an intraplate signature. A thorough search at Crater Lake failed to provide any evidence for an intraplate signature (Bacon 1990, and unpubl. data); data available for the Shasta area are insufficient for any conclusion. The intraplate component does not lead to high $^{87}Sr/^{86}Sr$ ratios or low ε_{Nd} values, as would be expected of old continental lithosphere. More likely, it is similar to OIB-source mantle, as suggested by Hughes (1990). A heterogeneous mixture of depleted and OIB-source mantle domains, enriched by a subduction component, has been identified as the source of arc lavas in many studies (*e.g.*, Morris & Hart 1983, Gill 1984, Hickey *et al.* 1986).

A possible answer to the question of how OIB-source-like mantle domains occur beneath the Cascades is that asthenosphere may rise locally east of the arc, such as beneath the Simcoe volcanic field, and become entrained in the westward flowing upper part of the wedge. Alternatively, OIB-source-like domains may be an integral part of the relatively young continental margin lithosphere. This lithosphere is composed of accreted oceanic and island-arc terranes, presumably including a mix of MORB- and OIB-source mantle, variously affected by Cenozoic and Mesozoic arc magmatism and related fluids. Lack of evidence for OIB-source mantle beneath Crater Lake results either from a failure of volcanism to sample it, perhaps because the volcanic zone is much narrower (~30 km) than in southern Washington or northern California (≥100 km), or to a real absence of OIB-source "plums" there.

In the part of the arc included in this study, the sub-arc lithosphere probably is Cenozoic in age north of Crater Lake and definitely contains crustal rocks at least as old as Paleozoic to the south, beneath Shasta and probably Lassen. It is in the last two areas of relatively old, and thus more "mature" crust, where we find isotopic evidence suggestive of contamination of some primitive lavas by crustal material.

Thermal structure

Eruption of HAOT implies that temperatures in the uppermost Cascade mantle are higher than indicated by traditional models of subduction zones (Baker *et al.* 1994). High temperatures at low pressures for separation of HAOT magma from the mantle required by phase-equilibrium studies (~1290°C at 11 kbar: Bartels *et al.* 1991), reinforced by the low pre-eruptive H_2O content of HAOT magmas (Sisson & Layne 1993), demand that the uppermost mantle beneath the Cascades is, at least locally, impressively hot. This is consistent with the youth of the subducting slab (Fig. 1), high heat flow (Blackwell *et al.* 1990), and extensional environment (Rogers 1985) of the southern Washington to northern California Cascades. The low $^{10}Be/^{9}Be$ ratios and B concentrations in the few published compositions of Cascade lavas also argue for a high-temperature thermal regime in comparison to many arcs (Leeman *et al.* 1990). As pointed out by Baker *et al.* (1994), magmas that give rise to arc basalt and basaltic andesite also must have traversed this same thermal regime, and owe their distinctive composition to melting of hydrous domains within it, although the temperature of last equilibration apparently was ~1200°C. They suggested that lower temperatures of last equilibration for arc basalt and basaltic andesite than for HAOT result from the steeper adiabatic melting curve for hydrous compositions, assuming onset of melting at a common depth of ~60 km.

The model presented by Baker *et al.* (1994) for the origin of magnesian lavas at Mount Shasta, which we believe applies to the primitive lavas of this study, calls upon adiabatic upwelling and melting of sub-arc mantle in the wedge that is locally enriched with variable amounts of a modern, hydrous subduction-derived component. Support for this hypothesis is found in the model of Furukawa (1993) for induced flow in the wedge owing to mechanical coupling with the subducting slab and in the observations by Zhao *et al.* (1994) of low *P*-wave velocities in the uppermost mantle beneath northern Honshu. Ongoing lithospheric extension in the northern California to southern Washington Cascades is consistent with mantle upwelling and promotes escape of primitive magmas. The required temperatures of 1200–1300°C virtually at the base of the Cascade crust must be transient, local phenomena, or the lower crust must be quite refractory, as otherwise voluminous crustal melts would be expected. Because HAOT has been erupted in the central Oregon Cascades from at least 7 Ma (Conrey *et al.* 1997; D.R. Sherrod, written comm., 1995), the uppermost mantle must have been gradually heated owing to relaxation of horizontal thermal gradients near local high-temperature regions. Although sustained temperatures as high as 1200–1300°C may not be everywhere characteristic of the uppermost mantle beneath the southern Washington to northern California Cascades, the mantle in this region is nonetheless anomalously hot.

ACKNOWLEDGEMENTS

We are pleased to acknowledge the contributions of the many chemists who produced the major-element, ICP, and INAA data of this study, especially D.F. Siems, S.T. Pribble, T.L. Fries, and J.N. Grossman. Advice and instruction in analysis by mass spectrometry were kindly provided to the second author by T.D. Bullen and J.L. Wooden. We thank L.H. Adami for measuring oxygen isotope ratios. W.K. Hart shared his unpublished data with us. Discussions with T.W. Sisson and J.B. Lowenstern helped us to refine our interpretations. Comments by Sisson and D.A. Clague on an early version of the manuscript led to many improvements. Journal reviews by M.B. Baker and T. Plank resulted in further clarification of the manuscript. We thank A.D. Johnston and G.T. Nixon for organizing the 1995 MAC symposium and for the opportunity to contribute to this thematic issue of *The Canadian Mineralogist.*

REFERENCES

ABBEY, S. (1983): Studies in "standard samples" of silicate rocks and minerals 1969–1982. *Geol. Surv. Can., Pap.* **83-15**.

ANDERSON, A.T., JR. (1974): Evidence for a picritic, volatile-rich magma beneath Mt. Shasta, California. *J. Petrol.* **15**, 243-267.

ARTH, J.G., BARKER, F., PETERMAN, Z.E. & FRIEDMAN, I. (1978): Geochemistry of the gabbro – diorite – tonalite – trondhjemite suite of southwest Finland and its implications for the origin of tonalitic and trondhjemitic magmas. *J. Petrol.* **19**, 289-316.

________ & HANSON, G.N. (1972): Quartz diorites derived by partial melting of eclogite or amphibolite at mantle depths. *Contrib. Mineral. Petrol.* **37**, 161-174.

BACON, C.R. (1990): Calc-alkaline, shoshonitic, and primitive tholeiitic lavas from monogenetic volcanoes near Crater Lake, Oregon. *J. Petrol.* **31**, 135-166.

________, GUNN, S.H., LANPHERE, M.A. & WOODEN, J.L. (1994): Multiple isotopic components in Quaternary volcanic rocks of the Cascade arc near Crater Lake, Oregon. *J. Petrol.* **35**, 1521-1556.

BAKER, M.B., GROVE, T.L., KINZLER, R.J., DONNELLY-NOLAN, J.M. & WANDLESS, G.A. (1991): Origin of compositional zonation (high-alumina basalt to basaltic andesite) in the Giant Crater lava field, Medicine Lake volcano, northern California. *J. Geophys. Res.* **96**, 21,819-21,842.

________, ________ & PRICE, R. (1994): Primitive basalts and andesites from the Mt. Shasta region, N. California: products of varying melt fraction and water content. *Contrib. Mineral. Petrol.* **118**, 111-129.

BARNES, C.G. (1992): Petrology of monogenetic volcanoes, Mount Bailey area, Cascade Range, Oregon. *J. Volcanol. Geotherm. Res.* **52**, 141-156.

BARTELS, K.S., KINZLER, R.J. & GROVE, T.L. (1991): High pressure phase relations of primitive high-alumina basalts from Medicine Lake volcano, northern California. *Contrib. Mineral. Petrol.* **108**, 253-270.

BEN OTHMAN, D., WHITE, W.M. & PATCHETT, J. (1989): The geochemistry of marine sediments, island arc magma genesis, and crust–mantle recycling. *Earth Planet. Sci. Lett.* **94**, 1-21.

BENZ, H.M., ZANDT, G. & OPPENHEIMER, D.H. (1992): Lithospheric structure of northern California from teleseismic images of the upper mantle. *J. Geophys. Res.* **97**, 4791-4807.

BLACKWELL, D.D., STEELE, J.L., FROHME, M.K., MURPHEY, C.F., PRIEST, G.R. & BLACK, G.L. (1990): Heat flow in the Oregon Cascade Range and its correlation with regional gravity, Curie Point depths, and geology. *J. Geophys. Res.* **95**, 19,475-19,493.

BLAKELY, R.J. & JACHENS, R.C. (1990): Volcanism, isostatic residual gravity, and regional tectonic setting of the Cascade volcanic province. *J. Geophys. Res.* **95**, 19,439-19,451.

________, ________, SIMPSON, R.W. & COUCH, R.W. (1985): Tectonic setting of the southern Cascade Range as interpreted from its magnetic and gravity fields. *Geol. Soc. Am., Bull.* **96**, 43-48.

BORG, L.E., CLYNNE, M.A. & BULLEN, T.D. (1997): The variable role of slab-derived fluids in the generation of a suite of primitive calc-alkaline lavas from the southernmost Cascades, California. *Can. Mineral.* **35**, 425-452.

BRANDON, A.D. & DRAPER, D.S. (1996): Constraints on the origin of the oxidation state of mantle overlying subduction zones: An example from Simcoe, Washington, USA. *Geochim. Cosmochim. Acta* **60**, 1739-1749.

BRENAN, J.M., SHAW, H.F., PHINNEY, D.L. & RYERSON, F.J. (1994): Rutile – aqueous fluid partitioning of Nb, Ta, Hf, Zr, U and Th: implications for high field strength element depletions in island-arc basalts. *Earth Planet. Sci. Lett.* **128**, 327-339.

BRUGGMAN, P.E., BACON, C.R., MEE, J.S., PRIBBLE, S.T. & SIEMS, D.F. (1989): Chemical analyses of volcanic rocks from monogenetic and shield volcanoes near Crater Lake, Oregon. *U.S. Geol. Surv., Open-File Rep.* **89-562**.

BULLEN, T.D. & CLYNNE, M.A. (1989): Coupled spatial, chemical, and isotopic characteristics of primitive lavas from the Lassen region, California. *In* Continental Magmatism Abstracts. *New Mexico Bur. Mines, Mineral Resources Bull.* **131**, 33.

________ & ________ (1990): Trace element and isotopic constraints on magmatic evolution at Lassen volcanic center. *J. Geophys. Res.* **95**, 19,671-19,691.

CARLSON, R.W. (1984): Isotopic constraints on Columbia River flood basalt genesis and the nature of the subcontinental mantle. *Geochim. Cosmochim. Acta* **48**, 2357-2372.

CARMICHAEL, I.S.E. (1991): The redox states of basic and silicic magmas: a reflection of their source regions? *Contrib. Mineral. Petrol.* **106**, 129-141.

CHRISTIANSEN, R.L., KLEINHAMPL, F.J., BLAKELY, R.J., TUCHEK, E.T., JOHNSON, F.L. & CONYAC, M.D. (1977): Resource appraisal of the Mount Shasta Wilderness Study Area, Siskiyou County, California. *U.S. Geol. Surv., Open-File Rep.* **77-250**.

CHURCH, S.E. (1976): The Cascade Mountains revisited: a re-evaluation in light of new lead isotopic data. *Earth Planet. Sci. Lett.* **29**, 175-188.

________, LEHURAY, A.P., GRANT, A.R., DELEVAUX, M.H. & GRAY, J.E. (1986): Lead-isotopic data from sulfide minerals from the Cascade Range, Oregon and Washington. *Geochim. Cosmochim. Acta* **50**, 317-328.

CLYNNE, M.A. (1990): Stratigraphic, lithologic, and major element geochemical constraints on magmatic evolution at Lassen volcanic center, California. *J. Geophys. Res.* **95**, 19,651-19,669.

________ (1993): *Geologic Studies of the Lassen Volcanic Center, Cascade Range, California.* Ph.D. thesis, Univ. of California at Santa Cruz, Santa Cruz, California.

________ & BORG, L.E. (1997): The composition of olivine and chromian spinel in primitive tholeiitic and calc-alkaline lavas from the Lassen area, southernmost Cascade Range, California: a reflection of relative source fertility. *Can. Mineral.* **35**, 453-472.

CONREY, R.M., SHERROD, D.R., HOOPER, P.R. & SWANSON, D.A. (1997): Diverse primitive magmas in the Cascade arc, northern Oregon and southern Washington. *Can. Mineral.* **35**, 367-398.

DONNELLY-NOLAN, J.M. (1988): A magmatic model of Medicine Lake volcano, California. *J. Geophys. Res.* **93**, 4412-4420.

________, CHAMPION, D.E., GROVE, T.L., BAKER, M.B., TAGGART, J.E. JR. & BRUGGMAN, P.E. (1991): The Giant Crater lava field: geology and geochemistry of a compositionally zoned, high-alumina basalt to basaltic andesite eruption at Medicine Lake volcano, California. *J. Geophys. Res.* **96**, 21,843-21,863.

DRUMMOND, M.S. & DEFANT, M.J. (1990): A model for trondhjemite – tonalite – dacite genesis and crustal growth via slab melting: Archean to modern comparisons. *J. Geophys. Res.* **95**, 21,503-21,521.

FUIS, G.S., ZUCCA, J.J., MOONEY, W.D. & MILKEREIT, B. (1987): A geologic interpretation of seismic-refraction results in northeastern California. *Geol. Soc. Am., Bull.* **98**, 53-65.

FURUKAWA, Y. (1993): Depth of the decoupling plate interface and thermal structure under arcs. *J. Geophys. Res.* **98**, 20,005-20,013.

GARDNER, C.A. (1994): Temporal, spatial and petrologic variations of lava flows from the Mount Bachelor volcanic chain, central Oregon High Cascades. *U.S. Geol. Surv., Open-File Rep.* **94-261**.

GERLACH, D.C. & GROVE, T.L. (1982): Petrology of Medicine Lake Highland volcanics: characterization of endmembers of magma mixing. *Contrib. Mineral. Petrol.* **80**, 147-159.

GILL, J.B. (1981): *Orogenic Andesites and Plate Tectonics.* Springer-Verlag, New York, N.Y.

________ (1984): Sr–Pb–Nd isotopic evidence that both MORB and OIB sources contribute to oceanic island arc magmas in Fiji. *Earth Planet. Sci. Lett.* **68**, 443-458.

GREEN, T.H. (1995): Significance of Nb/Ta as an indicator of geochemical processes in the crust–mantle system. *Chem. Geol.* **120**, 347-359.

GROVE, T.L., KINZLER, R.J., BAKER, M.B., DONNELLY-NOLAN, J.M. & LESHER, C.E. (1988): Assimilation of granite by basaltic magma at Burnt Lava flow, Medicine Lake volcano, northern California: decoupling of heat and mass transfer. *Contrib. Mineral. Petrol.* **99**, 320-343.

GUFFANTI, M. & WEAVER, C.S. (1988): Distribution of Late Cenozoic vents in the Cascade Range: volcanic arc segmentation and regional tectonic considerations. *J. Geophys. Res.* **93**, 6513-6529.

HARMON, R.S. & HOEFS, J. (1995): Oxygen isotope heterogeneity of the mantle deduced from global ^{18}O systematics of basalts from different geotectonic settings. *Contrib. Mineral. Petrol.* **120**, 95-114.

HART, S.R. (1984): A large-scale isotope anomaly in the southern hemisphere mantle. *Nature* **309**, 753-757.

HART, W.K., ARONSON, J.L. & MERTZMAN, S.A. (1984): Areal distribution and age of low-K, high-alumina olivine tholeiite magmatism in the northwestern Great Basin: *Geol. Soc. Am., Bull.* **95**, 186-195.

HICKEY, R.L., FREY, F.A., GERLACH, D.C. & LOPEZ-ESCOBAR, L. (1986): Multiple sources for basaltic arc rocks from the southern volcanic zone of the Andes (34°–41°S): trace element and isotopic evidence for contributions from subducted oceanic crust, mantle, and continental crust. *J. Geophys. Res.* **91**, 5963-5983.

HILDRETH, W. & FIERSTEIN, J. (1995): Geologic map of the Mount Adams volcanic field, Cascade Range of southern Washington. *U.S. Geol. Surv., Map* **I-2460** (scale 1:50,000).

________ & LANPHERE, M.A. (1994): Potassium–argon geochronlogy of a basalt – andesite – dacite arc system: the Mount Adams volcanic field, Cascade Range of southern Washington. *Geol. Soc. Am., Bull.* **106**, 1413-1429.

HOLE, M.J., SAUNDERS, A.D., MARRINER, G.F. & TARNEY, J. (1984): Subduction of pelagic sediments: implications for the origin of Ce-anomalous basalts from the Mariana Islands. *J. Geol. Soc. Lond.* **141**, 453-472.

HUGHES, S.S. (1990): Mafic magmatism and associated tectonism of the central High Cascade Range, Oregon. *J. Geophys. Res.* **95**, 19,623-19,638.

________ & TAYLOR, E.M. (1986): Geochemistry, petrogenesis, and tectonic implications of central High Cascade mafic platform lavas. *Geol. Soc. Am., Bull.* **97**, 1024-1036.

IONOV, D.A., PRIKHOD'KO, V.S. & O'REILLY, S.Y. (1995): Peridotite xenoliths in alkali basalts from the Sikhote–Alin, southeastern Siberia, Russia: trace-element signatures of mantle beneath a convergent continental margin. *Chem. Geol.* **120**, 275-294.

ITO, E. & STERN, R.J. (1985/86): Oxygen- and strontium-isotopic investigations of subduction zone volcanism: the case of the Volcano Arc and the Marianas Island Arc. *Earth Planet. Sci. Lett.* **76**, 312-320.

LANGMUIR, C.H., BENDER, J.F., BENCE, A.E., HANSON, G.N. & TAYLOR, S.R. (1977): Petrogenesis of basalts from the FAMOUS area: Mid-Atlantic Ridge. *Earth Planet. Sci. Lett.* **36**, 133-156.

LEAVER, D.S., MOONEY, W.D. & KOHLER, W.M. (1984): A seismic refraction study of the Oregon Cascades. *J. Geophys. Res.* **89**, 3121-3134.

LEEMAN, W.P., SMITH, D.R., HILDRETH, W., PALACZ, Z. & ROGERS, N. (1990): Compositional diversity of late Cenozoic basalts in a transect across the southern Washington Cascades: implications for subduction zone magmatism. *J. Geophys. Res.* **95**, 19,561-19,582.

LUHR, J.F. (1992): Slab-derived fluids and partial melting in subduction zones: insights from two contrasting Mexican volcanoes (Colima and Ceboruco). *J. Volcanol. Geotherm. Res.* **54**, 1-18.

MARTIN, H. (1987): Petrogenesis of Archaean trondhjemites, tonalites, and granodiorites from eastern Finland: major and trace element geochemistry. *J. Petrol.* **28**, 921-953.

MATTEY, D., LOWRY, D. & MACPHERSON, C. (1994): Oxygen isotope composition of mantle peridotite. *Earth Planet. Sci. Lett.* **128**, 231-241.

McCulloch, M.T. & Gamble, J.A. (1991): Geochemical and geodynamical constraints on subduction zone magmatism. *Earth Planet. Sci. Lett.* **102**, 358-374.

McDonough, W.F. & Frey, F.A. (1989): Rare earth elements in upper mantle rocks. *In* Geochemistry and Mineralogy of Rare Earth Elements (B.R. Lipin & G.A. McKay, eds.). *Rev. Mineral.* **21**, 99-145.

Miller, D.M., Goldstein, S.L. & Langmuir, C.H. (1994): Cerium/lead and lead isotope ratios in arc magmas and the enrichment of lead in the continents. *Nature* **368**, 514-519.

Mooney, W.D. & Weaver, C.S. (1989): Regional crustal structure and tectonics of the Pacific coastal states; California, Oregon, and Washington. *In* Geophysical Framework of the Continental United States (L.C. Pakiser & W.D. Mooney, eds.). *Geol. Soc. Am., Mem.* **172**, 129-161.

Morris, J.D. & Hart, S.R. (1983): Isotopic and incompatible element constraints on the genesis of island arc volcanics from Cold Bay and Amak Island, Aleutians, and implications for mantle structure. *Geochim. Cosmochim. Acta* **47**, 2015-2030.

________ & Tera, F. (1989): ^{10}Be and ^{9}Be in mineral separates and whole rocks from volcanic arcs: implications for sediment subduction. *Geochim. Cosmochim. Acta* **53**, 3197-3206.

Muffler, L.J.P. & Tamanyu, S. (1995): Tectonic, volcanic, and geothermal comparison of the Tohoku volcanic arc (Japan) and the Cascade volcanic arc (USA). Proceedings of the World Geothermal Congress (Florence, Italy), International Geothermal Assoc. (725-730).

Nye, C.J. & Reid, M.R. (1986): Geochemistry of primary and least fractionated lavas from Okmok volcano, central Aleutians: implications for arc magma genesis. *J. Geophys. Res.* **91**, 10,271-10,287.

Plank, T. & White, W. (1995): Nb and Ta in arc and mid-ocean ridge basalts. *Eos (Trans. Am. Geophys. Union)* **76**(46), F655 (abstr.).

Rapp, R.P & Watson, E.B. (1995): Dehydration melting of metabasalt at 8–32 kbar: implications for continental growth and crust–mantle recycling. *J. Petrol.* **36**, 891-931.

Riddihough, R., Finn, C. & Couch, R. (1986): Klamath – Blue Mountain lineament, Oregon. *Geology* **14**, 528-531.

Rogers, G.C. (1985): Variation in Cascade volcanism with margin orientation. *Geology* **13**, 495-498.

Rudnick, R.L. (1995): Making continental crust. *Nature* **378**, 571-578.

________ & Goldstein, S.L. (1990): The Pb isotopic compositions of lower crustal xenoliths and the evolution of lower crustal Pb. *Earth Planet. Sci. Lett.* **98**, 192-207.

Sisson, T.W. & Layne, G.D. (1993): H_2O in basalt and basaltic andesite glass inclusions from four subduction-related volcanoes. *Earth Planet. Sci. Lett.* **117**, 619-635.

Sobolev, A.V. & Chaussidon, M. (1996): H_2O concentrations in primary melts from supra-subduction zones and mid-ocean ridges: implications for H_2O storage and recycling in the mantle. *Earth Planet. Sci. Lett.* **137**, 45-55.

Stern, R.A., Hanson, G.N. & Shirey, S.B. (1989): Petrogenesis of mantle-derived, *LILE*-enriched Archean monzodiorites and trachyandesites (sanukitoids) in southwestern Superior Province. *Can. J. Earth Sci.* **26**, 1688-1712.

Stolper, E. & Newman, S. (1994): The role of water in the petrogenesis of Mariana trough magmas. *Earth Planet. Sci. Lett.* **121**, 293-325.

Sun, Shen-Su & McDonough, W.F. (1989): Chemical and isotopic systematics of oceanic basalts: implications for mantle composition and processes. *In* Magmatism in the Ocean Basins (A.D. Saunders & M.J. Norry, eds.). *Geol. Soc., Spec. Publ.* **42**, 313-345.

Taylor, S.R. & McLennan, S.M. (1995): The geochemical evolution of the continental crust. *Rev. Geophys.* **33**, 241-265.

Trehu, A.M., Asudeh, I., Brocher, T.M., Luetgert, J.H., Mooney, W.D., Nabelek, J.L. & Nakamura, Y. (1994): Crustal architecture of the Cascadia forearc. *Science* **266**, 237-243.

Wagner, T.P., Donnelly-Nolan, J.M. & Grove, T.L. (1995): Evidence of hydrous differentiation and crystal accumulation in the low-MgO, high-Al_2O_3 Lake Basalt from Medicine Lake volcano, California. *Contrib. Mineral. Petrol.* **121**, 201-216.

Walker, G.W. & MacLeod, N.S. (1991): Geologic map of Oregon. *U.S. Geol. Surv., Map* (scale 1:500,000).

Wells, R.E. & Heller, P.L. (1988): The relative contribution of accretion, shear, and extension to Cenozoic tectonic rotation in the Pacific Northwest. *Geol. Soc. Am., Bull.* **100**, 325-338.

White, W.M., Hofmann, A.W. & Puchelt, H. (1987): Isotope geochemistry of Pacific mid-ocean ridge basalt. *J. Geophys. Res.* **92**, 4881-4893.

________ & Patchett, J. (1984): Hf–Nd–Sr isotopes and incompatible element abundances in island arcs: implications for magma origins and crust–mantle evolution. *Earth Planet. Sci. Lett.* **67**, 167-185.

Woodhead, J.D., Harmon, R.S. & Fraser, D.G. (1987): O, S, Sr, and Pb isotope variations in volcanic rocks from the Northern Mariana Islands: implications for crustal recycling in intra-oceanic arcs. *Earth Planet. Sci. Lett.* **83**, 39-52.

Zhao, D., Hasegawa, A. & Kanamori, H. (1994): Deep structure of Japan subduction zone as derived from local, regional, and teleseismic events. *J. Geophys. Res.* **99**, 22,313-22,329.

Received December 19, 1995, revised manuscript accepted November 12, 1996.